24339-H005-R0-00

ASTP RANGING SYSTEM
MATHEMATICAL MODEL DEVELOPMENT

ASTP RANGING SYSTEM
MATHEMATICAL MODEL
FINAL REPORT

NAS 9-13296

4 October 1973

Prepared for
NATIONAL AERONAUTICS AND SPACE ADMINISTRATION
JOHNSON SPACE CENTER
HOUSTON, TEXAS

Prepared by
Electronic Systems Engineering Department

TRW
SYSTEMS GROUP

24339-H005-R0-00

ASTP RANGING SYSTEM

MATHEMATICAL MODEL DEVELOPMENT

ASTP RANGING SYSTEM
MATHEMATICAL MODEL
FINAL REPORT

NAS 9-13296

4 October 1973

Prepared for
NATIONAL AERONAUTICS AND SPACE ADMINISTRATION
JOHNSON SPACE CENTER
HOUSTON, TEXAS

Prepared by

M. R. Ellis
L. H. Robinson

Approved by: 

L. H. Robinson, Jr., Program Manager

Approved by: 

G. R. Shook, Manager
Electronic Systems Engineering Department

TRW
SYSTEMS GROUP

CONTENTS

ILLUSTRATIONS

TABLES

1. INTRODUCTION

This report concludes a six month study project to develop a mathematical model of the VHF ranging system. This model will be used to analyze the performance of the ranging system of the Apollo-Soyuz Test Project (ASTP).

The objective of this study has been attained in the following manner: the operation of the Apollo VHF ranging system (which has been adapted for use in the ASTP) was carefully reviewed, existing models of the various aspects of the ranging system were reviewed, and the modelling approaches to be used in this study were selected.

The results of the study, which was separated into five specific tasks, were presented in Inter-Office Memoranda which accompanied monthly progress reports. These detailed technical descriptions of each task are presented as appendices to this report. Task divisions were as follows:

1) Task 1, Early Late Gate Model Development,

2) Task 2, Unlock Probability Development,

3) Task 3, System Error Model Development,

4) Task 4, Probability of Acquisition and Acquisition Model Development, and

5) Task 5, Math Model Validation Testing.

By combining the results of each task, a complete mathematical model of the VHF ranging system was developed.

Section 2 of this report presents the ranging system mathematical model in block diagram form, and also includes a brief description of the overall model. In Section 3, a procedure for implementing the math model is presented. Section 4 includes a discussion of the validation of the math model, and Section 5 presents the overall summary and conclusions of the study effort.

The overall objectives of the tasks have been satisfied by the development of the model presented in this report. The mathematical model developed in this study extends the knowledge of the VHF ranging system and increases the capability for analyzing the ranging system.

2. THE VHF RANGING SYSTEM MATHEMATICAL MODEL

The mathematical model presented in this report includes information extracted from TRW reports by Chang, Eisenhauer and Ridge (References 1, 2) and the RCA Critical Design Reviews (References 3 and 4). Also information generated by Stiffler (Reference 5) and Goldman (Reference 6) is used as a basis for the acquisition model.

This section gives a general description of the mathematical model. The detailed technical descriptions of each element of the model are given in Appendices A through D.

2.1 BLOCK DIAGRAM OF THE RANGING MATHEMATICAL MODEL

A block diagram of the mathematical model of the ASTP ranging system has been created (see Figure 2-1) to show the primary calculations which are required to perform an analysis. This block diagram is not intended to accurately trace signal flow through the communications link, but, rather, is presented to show the important input parameters used and to present the mathematical relationships required for a complete analysis. Table 2-1 gives the definition of each symbol used in the block diagram.

2.1.1 Block Diagram

The block diagram presented in Figure 2-1 is included in this report as a map which shows the operations required in the computation of the ASTP VHF ranging system performance. The mathematical derivations and assumptions upon which equations are based are given in the Appendices to this report.

2.1.2 Description of the Soyuz Math Model

The section of the block diagram (Figure 2-1) to the left of the dashed line shows the major elements required in the analysis of the Soyuz ranging equipment.

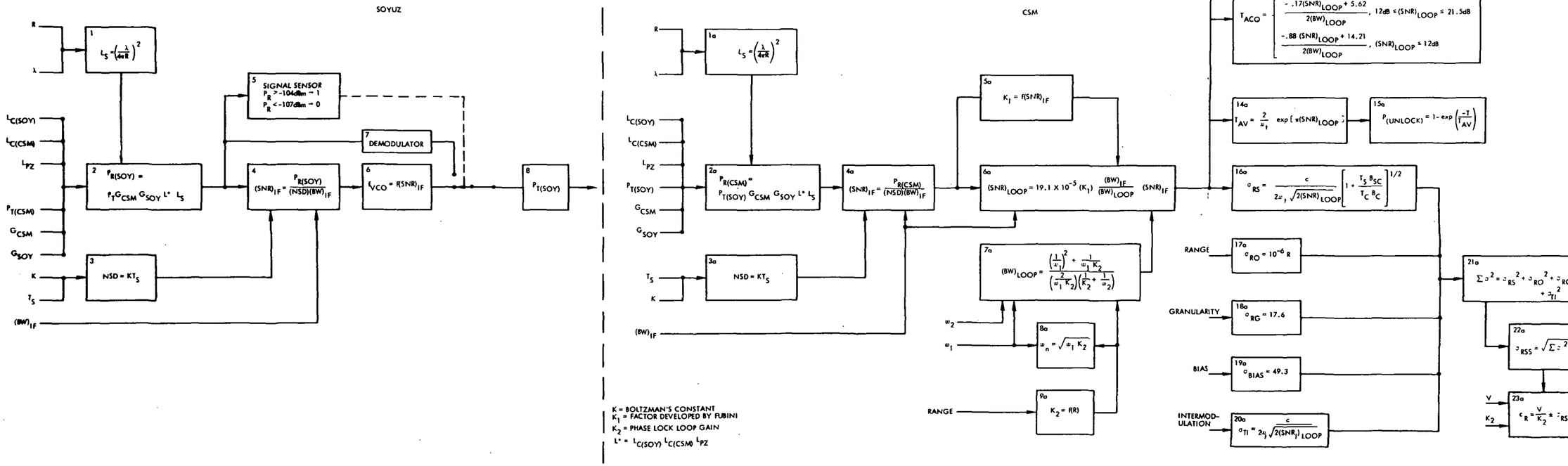

Figure 2-1. Mathematical Model of the VHF Ranging System

Table 2-1. Definition of Terms

$(BW)_{IF}$	noise bandwidth of the receiver IF
$(BW)_{loop}$	noise bandwidth of the tracking loop
c	speed of light
$G_{(CSM)}$, $G_{(SOY)}$	antenna gain of the CSM and Soyuz respectively
K	Boltzman's constant
K_1	envelope detector degradation factor
K_2	phase lock loop gain
$L_{c(CSM)}$, $L_{c(SOY)}$	circuit loss, CSM and Soyuz, respectively
L_{pz}	polarization loss
L_s	space loss
L*	combined circuit losses (L_c) and polarization loss
NSD	noise spectral density
$P_{R(CSM)}$, $P_{R(SOY)}$	received power at the CSM and Soyuz respectively
$P_{(UNLOCK)}$	probability of unlock
R	range
$(SNR)_{IF}$	IF signal to noise ratio
$(SNR)_{loop}$	loop signal to noise ratio (noise is the result of receiver thermal characteristics)
$(SNR_I)_{loop}$	loop signal to noise ratio (noise is the result of intermodulation of voice and ranging signals)

Table 2-1. Definition of Terms (Continued)

V	steady state velocity
σ_{BIAS}	range error due to bias
σ_{RG}	range error due to granularity
σ_{RO}	range error due to oscillator instability
σ_{RS}	range error due to thermal noise
σ_{RSS}	square root of the sum of the squares of errors from all sources
σ_{TI}	range error due to simultaneous (Soyuz to CSM) voice and ranging
ω_1	first filter break frequency
ω_2	second filter break frequency
ω_n	natural loop frequency
ω_t	tone frequency
θ_d	signal phase shift resulting from the two way transmission of ranging information between the CSM and Soyuz

An explanation of each block of the Soyuz system is as follows:

1) Block 1

Block 1 presents the equation necessary to compute space loss which is a function of distance the r.f. signal has to traverse and the carrier frequency of the signal.

2) Block 2

Block 2 presents the equations necessary to compute the power available at the Soyuz receiver front end as a result of the transmission of a VHF carrier from the CSM.

3) Block 3

Block 3 presents the equations necessary to compute the receiver noise spectral density.

4) Block 4

Block 4 presents the equations necessary to compute the Soyuz receiver IF signal to noise ratio.

5) Block 5

Block 5 is a representation of the Soyuz signal sensor which senses the received power level. Based on the received signal level, the signal sensor performs the switching functions which cause the Soyuz receiver to perform the steps required in ranging signal acquisition.

6) Block 6

Block 6 shows that the frequency of the Soyuz phase lock VCO is related to the received signal. The VCO output modulates the Soyuz transmitter.

7) Block 7

Block 7 represents the demodulation, which detects the coarse and mid-tones and routes the detected signal to the transmitter.

8) Block 8

Block 8 represents the Soyuz transmitter, which during the ranging operation transmits a signal with a finite signal to noise ratio, as described in the Math Model Implementation (Section 3).

2.1.3 Description of the CSM Math Model

The CSM as described in Appendix A initiates the ranging sequence, and upon successful completion of the acquisition process measures and displays range information.

The section of the block diagram (Figure 2-1) to the right of the dashed line shows the major elements required in the analysis of the CSM ranging system.

An explanation of each element of the block diagram of the CSM ranging system is as follows:

1) Block 1a

   Block 1a presents the equation necessary to compute space loss which is a function of distance the r.f. signal has traversed and the carrier frequency of the transmitted signal.

2) Block 2a

   Block 2a presents the equation necessary to compute the power available at the CSM receiver front end as a result of the transmission of a VHF carrier from the Soyuz.

3) Block 3a

   Block 3a presents the equation necessary to compute the receiver noise spectral density.

4) Block 4a

   Block 4a presents the equation necessary to compute the CSM receiver IF signal to noise ratio.

5) Block 5a

   Block 5a indicates the computation of the degradation in signal to noise ratio resulting from the use of envelope detection in the phase lock loop.

6) Block 6a

   Block 6a presents the relationship between IF signal to noise ratio and phase lock loop signal to noise ratio.

7) Block 7a

   Block 7a presents the equation by which the CSM phase lock loop bandwidth may be computed

8) Block 8a

Block 8a gives the relationship between loop natural frequency and other loop parameters.

9) Block 9a

Block 9a presents the relationship which allows loop gain to be determined.

10) Blocks 10a, 11a, and 12a

Blocks 10a, 11a, and 12a show the equations by which phase difference may be converted to range and range rate.

11) Block 13a

Block 13a presents the mathematical relationships by which loop signal to noise ratio and bandwidth may yield the loop acquisition time (see Appendix D).

12) Blocks 14a and 15a

Blocks 14a and 14a allow the computation of unlock probability.

13) Blocks 17a, 18a, 19a, and 20a

Blocks 17a, 18a, 19a, and 20a present range error values resulting from oscillator instability, readout granularity, bias, and intermodulation.

14) Block 21a

Block 21a shows the summation of the squares of values obtained from various error sources.

15) Block 22a

Block 22a presents the square root of the sum of the squares of various error values giving a root of the sum of the squares (r.s.s) error.

16) Block 23a

Block 23a shows the calculation of range error which is the summing of the error resulting from spacecraft motion with the r.s.s of all other error sources.

3. MATHEMATICAL MODEL IMPLEMENTATION

Utilization and proper validation of the math model presented in this report requires an orderly procedure for evaluating the various portions of the model. Such an implementation of the model can be separated into functional modules or building blocks, following the outline of model formulation presented in the appendices. In this manner, as more accurate or realistic model elements are developed, through more extensive analytical investigation or experiment validation, the currently used model elements may be replaced without altering other parts of the overall model implementation. While the following development parallels the model presentation in the appendices, in several instances additional modelling has been required, to provide an orderly computational progression from one portion of the model to the next.

In the following paragraphs is outlined a procedure for implementing 1) the propagation equation, which relates received power through trajectory-dependent relationships to the range between the vehicles, 2) the receiver noise effects, from which IF signal to noise ratios are determined, 3) the ranging turnaround and associated tracking loop parameters, which yield loop gains, bandwidths, and signal to noise ratios, 4) unlock time and probability of unlock, 5) range errors and probability of correct range measurement, and 6) acquisition time and probability of acquisition. The implementation is divided into two overall categories: 1) ranging only, and 2) simultaneous voice and ranging operation, which are further subdivided into operation using 1) restricted antenna coverage region parameters (corresponding to CSM to Soyuz look angles of $\theta=35°\pm10°$ and $\phi=180°\pm10°$ and Soyuz to CSM look angles of $\theta=10°\pm5°$ and $\phi=180°\pm5°$, or 2) nominal 80% antenna coverage region parameters. The restricted antenna coverage is the expected operating zone during ASTP rendezvous.

3.1 GENERAL NUMERICAL CONSIDERATIONS

When contemplating a numerical implementation of a complicated math model, several overall considerations influence the specific form of the implementation. First, the common circuit margin practice of combining power values in dBm (or dBw) and other factors in dB can lead to significant numerical errors (truncation, when using a digital computer) if the parameters involved have widely differing values. The preferred numerical approach performs multiplication and division of linear quantities instead of addition and subtraction of logarithmic quantities, thereby retaining numerical precision to a much greater degree.

A second consideration is that a great many parameters in the model are ultimately trajectory-dependent. While specific trajectory data is not presently available, nominal trajectory assumptions can be made to provide a defining link among these portions of the model. A manifestation of this approach, for example, is to separate out range-independent effects; such effects can then be precalculated for a given set of trajectory assumptions, leaving only variation with range as the net independent effect.

Third, many of the formulas presented for various portions of the model are based on approximations which may not precisely fit specified or measured parameter values. If the functional forms given are assumed to be representative of the specific processes involved, and if these formulas are desired to yield the given data, then correction factors may be required. In such cases, the model could be improved if a series of measurements could be made on the equipment, so that piecewise-linear or other suitable parameteric curves could be substituted for the formulas.

3.2 RANGING ONLY IMPLEMENTATION

In many instances, a modelling formula can be factored so that constant coefficients, independent of variations in received power or at least range loss, are obtained. By precomputing those coefficients,

the effects of truncation errors being propagated from one computation to the next may be minimized, particularly if double precision arithmetic is used. There will be no great penalty in computation time, since these coefficients are computed only once for a given trajectory assumption. A great savings in overall computation time can be realized by incorporating the precalculated coefficients in single precision range-variable computations.*

Those coefficients and factors which lend themselves to precalculation are propagation effects, receiver noise effects, and tracking loop factors. A basic assumption here is that the spacecraft-to-spacecraft line-of-sight (i.e., θ and ϕ look angles) remain constant throughout the trajectory so that all propagation effects except range loss remain constant. The following model implementation attempts to factor out meaningful precalculatable coefficients, starting with trajectory-dependent propagation effects.

3.2.1 Vehicle-to-Vehicle Propagation

The primary independent variable in the ranging system model is received power, since most of the modelled effects depend directly upon the strength of the received ranging signals. Other auxiliary parameters such as range, received power to noise spectral density ratio, and IF and loop signal to noise ratios are also important, but these parameters must be calculated ultimately from the received power. The logical starting point in the ranging system model implementation is the propagation equation

$$P_R = P_T L_T G_T L_S L_P G_R L_R \ , \qquad (3.2\text{-}1)$$

*Precalculated parameter values are given to eight significant figures herein, to avoid the effects of truncation errors on such computers as the Univac 1108; for the Control Data 6500, 15 digits would be required to retain full precision.

where for the linear form shown,

P_R = total received power at Soyuz or CSM (average or rms, milliwatts)

P_T = power transmitted from CSM or Soyuz (average modulated, milliwatts)

L_T = CSM or Soyuz transmit circuit losses (linear)

G_T = CSM or Soyuz transmit antenna gain (linear)

L_S = space loss = $\lambda^2/(4\pi R)^2$

λ = CSM or Soyuz transmitted carrier wavelengths (meters) = c/f

c = velocity of light in a vacuum = 2.997925×10^8 meters/sec.

f = CSM or Soyuz transmitted carrier frequency (Hz)

R = CSM-Soyuz range (separation distance, meters)

L_P = antenna-to-antenna polarization loss (linear)

G_R = Soyuz or CSM receive antenna gain (linear), and

L_R = Soyuz or CSM receive circuit losses(linear).

Note that there are two versions of Equation (3.2-1), one for CSM to Soyuz and the other for Soyuz to CSM. The common factor between the two received powers is the vehicle-to-vehicle range R, which as shown would appear to be the independent variable in Equation (3.2-1). But the antenna gains and polarization losses are functions of antenna geometry (radiation patterns) and the relative attitude time history of the spacecraft. Only if the line-of-sight between the vehicles is assumed constant, and the receive circuit losses are assumed independent of received signal level, will the space loss L_S remain the only trajectory-dependent factor, or specifically will the range loss contribution be the only variable in Equation (3.2-1).

If the effect of space loss is factored out, Eq. (3.2-1) becomes

$$P_R = PR1 \cdot L_S \,, \qquad (3.2\text{-}2)$$

where

$$PR1 = P_T L_T G_T L_P G_R L_R \ . \qquad (3.2\text{-}3)$$

Reference 7 lists values for the elements of (3.2-3) as

Carrier frequency

Soyuz 296.8 MHz

CSM 259.7 MHz

Transmit power (average modulated)

Soyuz 5 watts : 37 dBm

CSM 5 watts : 37 dBm

Transmit and receive circuit loss

Soyuz 3.8 dB

CSM 4.5 dB

Transmit and receive antenna gain

Soyuz -3 dB (restricted region) or -5 dB (80% coverage)

CSM -1 dB (restricted region) or -3 dB (80% coverage)

Antenna polarization

Soyuz RCP

CSM Linear

The assumed antenna-to-antenna polarization loss is

3 dB (restricted region) or 5 dB (80% coverage).

Incorporating this data into Equation (3.2-3), the precalculated values of average received power excluding space loss are

$$PR1_{CSM} = PR1_{Soyuz} = \begin{cases} 147.91084 \text{ mw (21.7 dBm), restricted region} \\ 37.153523 \text{ mw (15.7 dBm)*, 80\% coverage} \end{cases} . \qquad (3.2\text{-}4)$$

*The specified system parameters yield a 6 dB difference between restricted and 80% coverage precalculated coefficients.

Factoring out the effect of range loss from the space loss,

$$L_S = LS1/R^2 = LS1 \cdot R_{LOSS}, \tag{3.2-5}$$

where

$$LS1 = \lambda^2/(4\pi)^2 = c^2/(4\pi f)^2 \tag{3.2-6}$$

and

$$R_{LOSS} = 1/R^2 . \tag{3.2-7}$$

Incorporating the frequency data into (3.2-6), the precalculated values of space loss excluding range loss are

$$LS1_{\substack{\text{Soyuz} \\ \text{to CSM}}} = 0.0064609147 \ (-21.897060 \text{ dB})$$

and (3.2-8)

$$LS1_{\substack{\text{CSM to} \\ \text{Soyuz}}} = 0.0084387457 \ (-20.737221 \text{ dB}) .$$

Substituting Equations (3.2-2) and (3.2-5) into (3.2-1),

$$P_R = PR1 \cdot LS1/R^2 = PR2 \cdot R_{LOSS}, \tag{3.2-9}$$

for which the precalculated values of average received power excluding range loss are

$$PR2_{Soyuz} = \begin{cases} 1.2481820 \text{ mw } (0.96277900 \text{ dBm}), \text{ restricted region} \\ 0.31352913 \text{ mw } (-5.0372210 \text{ dBm})^*, \text{ 80\% coverage} \end{cases}$$

and (3.2-10)

$$PR2_{CSM} = \begin{cases} 0.95563931 \text{ mw } (-0.19705994 \text{ dBm}), \text{ restricted region} \\ 0.24004574 \text{ mw } (-6.1970599 \text{ dBm})^*, \text{ 80\% coverage.} \end{cases}$$

---

*The specified system parameters yield a 6dB difference between restricted and 80% coverage precalculated coefficients.

Using the precalculated parameters, the range loss as a function of average received power at the CSM is

$$R_{LOSS} = 1/R^2 = P_{R_{CSM}}/PR2_{CSM} , \qquad (3.2\text{-}11)$$

where

$P_{R_{CSM}}$ = CSM average received power (mw), and

$PR2_{CSM}$ = restricted or 80% precalculated values (mw) from (3.2-10).

An entirely equivalent definition of range loss in terms of Soyuz average received power is

$$R_{LOSS} = P_{R_{Soyuz}}/PR2_{Soyuz} , \qquad (3.2\text{-}12)$$

where either the restricted or 80% Soyuz value from (3.2-10) is used. Given the average received power at one vehicle, the average received power at the other vehicle can be obtained from

$$P_{R_{Soyuz}} = PR2_{Soyuz} \cdot R_{LOSS} \qquad (3.2\text{-}13)$$

or

$$P_{R_{CSM}} = PR2_{CSM} \cdot R_{LOSS} , \qquad (3.2\text{-}14)$$

and the corresponding range (meters) is

$$R = 1/\sqrt{R_{LOSS}} . \qquad (3.2\text{-}15)$$

Equations (3.2-11) through (3.2-15) constitute the implementation of the propagation portion of the ranging system model. If a separate tabulation of space loss is desired, Equation (3.2-5) can be added to the implementation.

3.2.2 Receiver Noise

The receiver thermal noise spectral density is given by

$$\phi = N_o = kT, \tag{3.2-16}$$

where

$\phi = N_o$ = thermal noise spectral density (mw/Hz)

k = Boltzman's constant = 1.38054×10^{-20} mw/°K-Hz, and

T = receiver or system equivalent thermal noise temperature (°K).

The receiver IF noise power (mw, rms) is given by

$$P_{N_{IF}} = \phi B_{IF} = N_o B_{IF} = kTB_{IF}, \tag{3.2-17}$$

where

B_{IF} = one-sided equivalent noise bandwidth of the IF (Hz).*

Reference 7 lists values for elements of Equations (3.2-16) and (3.2-17) as

System noise temperature

Soyuz	1200°K
CSM	1200°K

IF noise bandwidth

Soyuz	70 kHz
CSM	70 kHz .

Incorporating these values in Equations (3.2-16) and (3.2-17), the

*Note that the value given for B_{IF} is a two-sided quantity when considered in baseband computations, such as the ratio of IF to loop bandwidths.

precalculated values of receiver noise spectral density are

$$N_{o_{CSM}} = N_{o_{Soyuz}} = 1.6566480 \times 10^{-17} \text{ mw/Hz}$$
$$= (-167.80770 \text{ dBm-logHz}) , \tag{3.2-18}$$

and the precalculated values of receiver IF noise power are

$$P_{N_{CSMIF}} = P_{N_{SoyuzIF}} = 1.1596536 \times 10^{-12} \text{ mw}$$
$$= (-119.35672 \text{ dBm}) . \tag{3.2-19}$$

Making use of the propagation precalculated factors, the average received power to noise spectral density ratio is

$$P_R/N_o = PRNO_1 \cdot R_{LOSS} , \tag{3.2-20}$$

where

$$PRNO1 = PR2/N_o . \tag{3.2-21}$$

Also, the IF signal to noise ratio is

$$SNR_{IF} = SNIF1 \cdot R_{LOSS} , \tag{3.2-22}$$

where

$$SNIF1 = PR2/P_{N_{IF}} . \tag{3.2-23}$$

Incorporating previously calculated factors, the precalculated values of P_R/N_o excluding range loss are

$$PRNO1_{Soyuz} = \begin{cases} 7.5343824 \times 10^{16} \text{ (168.77048 dB), restricted region} \\ 1.8925513 \times 10^{16} \text{ (162.77048 dB), 80\% coverage} \end{cases}$$

and (3.2-24)

$$PRNO1_{CSM} = \begin{cases} 5.7685115 \times 10^{16} \text{ (167.61064 dB), restricted region} \\ 1.4489846 \times 10^{16} \text{ (161.61064 dB), 80\% coverage} , \end{cases}$$

and the precalculated values of IF signal to noise ratio excluding range loss are

$$SNIF1_{Soyuz} = \begin{cases} 1.0763403 \times 10^{12} \text{ (120.31950 dB), restricted region} \\ 2.7036447 \times 10^{11} \text{ (114.31950 dB), 80\% coverage} \end{cases}$$

and (3.2-25)

$$SNIF1_{CSM} = \begin{cases} 8.2407308 \times 10^{11} \text{ (119.15966 dB), restricted region} \\ 2.0699780 \times 10^{11} \text{ (113.15966 dB), 80\% coverage .} \end{cases}$$

Equation (3.2-22) constitutes the implementation of the receiver noise model for the fine tone ranging case. If P_R/N_o values are also desired, Equation (3.2-20) can be added to the implementation.

3.2.3 Mid and Coarse Tone Receiver Noise Considerations

Equation (3.2-23) assumes that the CSM transmits a noiseless ranging signal to the Soyuz and that the Soyuz transmits a noiseless signal (i.e., all of the transmitted power P_T is devoted to signal). This may be a valid assumption for the case of fine tone tracking, but is unrealistic while the mid or coarse ranging tones are being relayed through the Soyuz. During acquisition, the Soyuz transponder is configured to directly turnaround the mid and coarse tones, and as shown in Figure A.2-6, the turnaround circuit consists primarily of the receiver, an envelope detector, a clipper, and the transmitter. In such a configuration, there will be some amount of retransmitted noise in addition to the retransmitted signal.

If the following symbol definitions are made:

SNR_{IFS} = Soyuz IF SNR, from (3.2-22)

SNR_{TS} = SNR transmitted from Soyuz

P_{TS} = total power transmitted from Soyuz (rms)

P_{TSS} = signal transmitted from Soyuz (rms)

P_{TNS} = noise transmitted from Soyuz (rms)

L_S = space loss, including antenna gains and circuit losses, etc.

P_{RC} = total power received at CSM (rms)

P_{RSC} = signal power received at CSM (rms)

P_{RNC} = noise power received at CSM (rms)

P_{NC} = thermal noise power in CSM (kTB_{IF})

SNR_{IFCX} = CSM IF SNR, excluding noise transmitted from Soyuz, from Equation (3.2-22), and

SNR_{IFC} = CSM IF SNR, including noise transmitted from Soyuz,

then the signal to noise ratio at the output of the Soyuz envelope detector is

$$SNR_{ENVS} = K_1(B_{IFS}/2B_{ENVS})\ SNR_{IFS}\ , \qquad (3.2\text{-}26)$$

where

K_1 = envelope detector degradation factor (see paragraph 3.2.7)

B_{IFS} = Soyuz IF bandwidth (cf., Equation 3.2-17), and

$2B_{ENVS}$ = two-sided audio bandwidth of the envelope detector.

Reference 4 specifies that the "input" amplifier following the envelope detector has a minimum one-sided bandwidth of 40 kHz, so there will be no bandwidth improvement in SNR*, and the bandwidth ratio in Equation (3.2-26) will be assumed to have a value of 1.0.

The clipper can be assumed to yield a 3 dB improvement in SNR, if half of the received noise (in-phase) is assumed to produce amplitude jitter at the output of the envelope detector, and the other half of the received noise (quadrature) is assumed to produce phase jitter.

*Recall, B_{IF} = 70 kHz.

Thus, the transmitted signal to noise ratio is twice that in Equation (3.2-26) or, dropping the bandwidth ratio factor,

$$SNR_{TS} = 2\ K_1\ SNR_{IFS}\ . \qquad (3.2\text{-}27)$$

Stating relationships between the transmitted signal and noise powers,

$$P_{TS} = P_{TSS} + P_{TNS} \qquad (3.2\text{-}28)$$

and

$$SNR_{TS} = P_{TSS}/P_{TNS}\ , \qquad (3.2\text{-}29)$$

so

$$P_{TNS} = P_{TS}/(SNR_{TS} + 1) \qquad (3.2\text{-}30)$$

and

$$P_{TSS} = P_{TS}\ SNR_{TS}/(SNR_{TS} + 1)\ . \qquad (3.2\text{-}31)$$

At the CSM,

$$SNR_{IFC} = P_{RSC}/(P_{NC}+P_{RNC}) = P_{TSS}L_S/(P_{NC}+P_{TNS}L_S)$$

$$= \frac{P_{TSS}/P_{TNS}}{(P_{NC}/P_{TNS}L_S)+1} = SNR_{TS}/[P_{NC}(SNR_{TS}+1)/P_{TS}L_S + 1]$$

$$= SNR_{TS}/[(SNR_{TS}+1)/(P_{RC}/P_{NC}) + 1] = SNR_{TS}/[(SNR_{TS}+1)/SNR_{IFCX} + 1]$$

$$SNR_{IFC} = \left(\frac{SNR_{TS}}{SNR_{TS}+SNR_{IFCX}+1}\right) SNR_{IFCX}\ , \qquad (3.2\text{-}32)$$

which should be used for the CSM IF SNR when computing system performance during acquisition of the mid and coarse tones.

Summarizing the mid and coarse tone cases (during acquisition), Equation (3.2-22) provides the Soyuz IF SNR for use with Equation (3.2-27)

and as input for calculating the Soyuz envelope detector degradation factor (see paragraph 3.2.7) in Equation (3.2-27). Equation (3.2-22) also supplies the CSM IF SNR (excluding noise transmitted from Soyuz) for use with (3.2-32). The resultant value from (3.2-32) takes the place of that from Equation (3.2-22) for the CSM IF SNR for the mid and coarse tone cases.

3.2.4 Tracking Loop Factors

Reference 1 assumes that tracking loop gain varies linearly in dB as range varies linearly and derives loop gain values based on data given in Table 3.1, obtained from References 3 and 4. No statement is made in the references whether the quoted power levels are peak or average, but ranging system operation has been discussed traditionally in terms of peak power. Also, Reference 8 quotes the value -107 dBm as being a NASA-supplied value for the average received power (with 5 watt average transmitted power) required for ranging acquisition; the tracking threshold following acquisition is listed as being 3 dB lower, at -110 dBm. These considerations lead to the assumption that the quoted power levels are peak.

The assumed functional variation of loop gain with range can be expressed as

$$\log_{10} K_L = aR + b \qquad (3.2\text{-}33)$$

or

$$K_L = 10^{aR+b} = 10^{aR} \cdot 10^{b} \quad , \qquad (3.2\text{-}34)$$

where

K_L = loop gain (linear), and

R = vehicle-to-vehicle range (in units yet to be assigned).

Table 3-1. APOLLO VHF TRACKING LOOP DESIGN PARAMETERS

RANGE (n.mi.)	MODULATION	CM RECEIVED RF LEVEL (dBm,peak)	LOOP	LOOP GAIN	LOOP NOISE BANDWIDTH (Hz.)*	ACQUISITION TIME (sec.)	LOOP BREAKPOINT FREQUENCIES (rad/sec)
200	RANGING ONLY	-107	CM FINE	20	0.975	2.33	0.1853, 2.27, 122.5
			CM MID	27.8	1.135	1.98	0.1853, 2.27, 122.5
			CM COARSE	315	7.42	0.319	0.63, 10.2, 250
			LM FINE	1720	21.6	>1	0.43, 18, 107
0.05	RANGING ONLY	-35	CM FINE	100	2.60	1.05	
			CM MID	139	3.41	0.89	
			CM COARSE	1575	27.0	0.142	
			LM FINE	8600	60.7	>0.5	
200	VOICE PLUS RANGING	-110	CM FINE	10	0.772		
			LM FINE	860	14		
0.05	VOICE PLUS RANGING	-38	CM FINE	50	1.59		
			LM FINE	4300	38.9		

* Noise bandwidth values are assumed to be one-sided

If R1 represents 0.05 n. mi., R2 represents 200 n. mi., and KL1 and KL2 represent the corresponding loop gains, Equation (3.2-33) can be manipulated to yield

$$a = \frac{\log KL1 - \log KL2}{R1-R2} = \frac{1}{R1-R2} \log \frac{KL1}{KL2} \qquad (3.2\text{-}35)$$

and

$$b = \log KL1 - aR1 = \log KL1 - \frac{R1}{R1-R2} \log \frac{KL1}{KL2} . \qquad (3.2\text{-}36)$$

Substituting Equations (3.2-35) and (3.2-36) into (3.2-33),

$$\log K_L = \frac{R}{R1-R2} \log \frac{KL1}{KL2} + \log KL1 - \frac{R1}{R1-R2} \log \frac{KL1}{KL2}$$

$$= \log \left[KL1 \left(\frac{KL1}{KL2} \right)^{\left(\frac{R-R1}{R1-R2} \right)} \right] \qquad (3.2\text{-}37)$$

or

$$K_L = KL1 \left(\frac{KL1}{KL2} \right)^{\left(\frac{R-R1}{R1-R2} \right)} . \qquad (3.2\text{-}38)$$

But loop gain is a function of received signal level, not range explicitly, so Equation (3.2-38) must be modified to show a functional dependence on received power instead of range. If Equation (3.2-9) is rewritten as

$$P_R = G^2/R^2 , \qquad (3.2\text{-}39)$$

where

$$G = R1\sqrt{PR1X} = R2\sqrt{PR2X} , \qquad (3.2\text{-}40)$$

PR1X = average received power at range R1, and

PR2X = average received power at range R2,

then

$$R = R1\sqrt{\frac{PR1X}{P_R}} = R2\sqrt{\frac{PR2X}{P_R}} \quad . \tag{3.2-41}$$

Substituting Equation (3.2-41) into (3.2-38),

$$K_L = KL1\left(\frac{KL1}{KL2}\right)^{\left(\frac{R1}{R1-R2}\right)\left(\sqrt{\frac{PR1X}{P_R}} - 1\right)} \quad . \tag{3.2-42}$$

The data values R1 = 0.05 n. mi., R2 = 200 n. mi., PR1X = -38 dBm, and PR2X = -110 dBm are not precisely compatible, due to roundoff of the specified values. One of the four values is a function of the other three and should be calculated. Assuming that the range values and PR2X are accurately specified,

$$PR1X = \left(\frac{R2}{R1}\right)^2 \quad PR2X = (-37.9588 \text{ dBm}) \tag{3.2-43}$$

To make Equation (3.2-42) compatible with the forms following Equation (3.2-9), so that range-independent parameters may be precalculated, if

$$SQPR2X = \sqrt{PR1X/PR2} \quad , \tag{3.2-44}$$

$$R1DR1M2 = R1/(R1-R2), \tag{3.2-45}$$

$$K1DK2 = KL1/KL2 \quad , \tag{3.2-46}$$

then

$$K_L = KL1(K1DK2)^{R1DR1M2 \cdot (SQPR2X \cdot R - 1)} \quad , \tag{3.2-47}$$

where R in this case is in meters. Note that the exponent in Equation (3.2-47) is independent of loop parameters and is also independent of whether CSM or Soyuz loops are involved. Thus, one exponent calculation is sufficient for all of the tracking loops.

Incorporating the data values specified above in Equations (3.2-44) through (3.2-46), the precalculated loop parameter values are

$$\begin{aligned} SQPR2X_{Apollo} &= 0.010799136^{*} \ , \\ SQPR2X_{ASTP} &= \begin{matrix} 0.012939366, \text{ restricted region} \\ 0.025817429, \text{ 80\% coverage} \end{matrix} \ , \\ R1DR1M2 &= -2.5006252 \times 10^{-4} \ , \text{ and} \\ K1DK2 &= 5, \text{ for all tracking loops} \ . \end{aligned} \qquad (3.2\text{-}48)$$

If loop gain can be assumed to be strictly a function of total received power, then Equation (3.2-47) constitutes the implementation of the loop gain portion of the ranging system model, with the following values for design loop gain

$$KL1 = \begin{cases} 100, \text{ CSM fine tone loop} \\ 139, \text{ CSM mid tone loop} \\ 1575, \text{ CSM coarse tone loop} \\ 8600, \text{ Soyuz fine tone loop} \end{cases} .$$

The subject of whether or not the loops operate on the net received signal power rather than total received power is discussed in paragraphs 3.2.5 and 3.3.1.

Reference 1 presents an approximate relationship between loop gain and the loop two-sided equivalent noise bandwidth:

$$2B_L = \frac{1/\omega_2^{\,2} + 1/\omega_1 K_L}{(2/\omega_1 K_L)(1/K_L + 1/\omega_2)} \ (\text{Hz}) \ , \qquad (3.2\text{-}49)$$

*Since this formulation is based on Apollo specifications, the exponent of Equation (3.2-28) can be factored as R1DR1M2 · (R/R1 - 1), so SQPR2X for Apollo is simply 1/R1, with R1 converted to meters. The differences between the Apollo and ASTP values for SQPR2X reflect different specifications for circuit loss, antenna gain, etc.

where K_L is the loop gain from Equation (3.2-47) and the ω's are the first two (of three) loop breakpoint frequencies. Rearranging for less computational complexity, Equation (3.2-49) can be written

$$2B_L = \frac{\omega_1 K_L/\omega_2{}^2 + 1}{2(1/K_L + 1/\omega_2)} \text{ (Hz)} . \qquad (3.2\text{-}50)$$

Due to the approximate nature of Equation (3.2-50), trial computations using the design loop gain values specified above do not yield the corresponding design loop bandwidth values. If the given functional form is assumed to be sufficiently representative of loop bandwidth variation with loop gain, then a correction must be applied to yield the design loop bandwidth values. The correction can assume the form

$$(2B_L)_{Actual} = X(2B_L)_{Calculated} + Y , \qquad (3.2\text{-}51)$$

where X and Y are the slope and intercept of a linear-type correction. If 2BL1 is the design value corresponding to loop gain KL1 (i.e., at range R1), 2BL2 corresponds to KL2, 2BLA is the value calculated substituting KL1 into Equation (3.2-50), and 2BLB is calculated using KL2, then

$$X = (2BL2 - 2BL1)/(2BLB - 2BLA) \qquad (3.2\text{-}52)$$

and

$$Y = 2BL2 - X \cdot 2BLB . \qquad (3.2\text{-}53)$$

The X and Y correction coefficients are different for the four loops.

Reference 1 also gives the loop natural resonant frequency as

$$\omega_n = \sqrt{\omega_1 K_L} \text{ (rad/sec)} \qquad (3.2\text{-}54)$$

and the loop damping factor as

$$\zeta = \frac{\omega_n}{2}\left(\frac{1}{K_L} + \frac{1}{\omega_2}\right) , \qquad (3.2\text{-}55)$$

where again these relationships are approximate, since only the first two loop breakpoint frequencies are used. For possible acquisition time considerations, the reciprocal loop natural resonant frequency (1/Hz) can be calculated using

$$1/f_n = 2\pi/\omega_n \, . \tag{3.2-56}$$

The specified and/or precalculatable parameters for loop bandwidth through damping factors are

$$\omega_1 = \begin{cases} 0.1853 \, , & \text{CSM fine tone loop} \\ 0.1853 \, , & \text{CSM mid tone loop} \\ 0.63 \, , & \text{CSM coarse tone loop} \\ 0.43 \, , & \text{Soyuz fine tone loop} \, , \end{cases}$$

$$1/\omega_2 = \begin{cases} 0.44052863 \, , & \text{CSM fine tone loop} \\ 0.44052863 \, , & \text{CSM mid tone loop} \\ 0.098039216 \, , & \text{CSM coarse tone loop} \\ 0.055555556 \, , & \text{Soyuz fine tone loop} \, , \end{cases}$$

$$1/\omega_2^2 = \begin{cases} 0.19406548 \, , & \text{CSM fine tone loop} \\ 0.19406548 \, , & \text{CSM mid tone loop} \\ 0.0096116878, & \text{CSM coarse tone loop} \\ 0.0030864198, & \text{Soyuz fine tone loop} \, , \end{cases} \tag{3.2-57}$$

$$X^* = \begin{cases} 0.48531950 \, , & \text{CSM fine tone loop} \\ 0.49450458 \, , & \text{CSM mid tone loop} \\ 0.50165178 \, , & \text{CSM coarse tone loop} \\ 0.47537755 \, , & \text{Soyuz fine tone loop} \, , \end{cases}$$

$$Y = \begin{cases} 0.24905032 \, , & \text{CSM fine tone loop} \\ 0.19474345 \, , & \text{CSM mid tone loop} \\ 0.42969329 \, , & \text{CSM coarse tone loop} \\ 15.401384 \, , & \text{Soyuz fine tone loop} \, . \end{cases}$$

*The X values given also include the 1/2 factor (cf. "2" in denominator) in Equation (3.2-50).

Equation (3.2-50), as modified in Equation (3.2-51) and Equations (3.2-54) through (3.2-56) constitute the remaining implementation of tracking loop factors. More complete measured data regarding loop gains, bandwidths, etc. could conceivably yield improved loop parameter modelling.

Tabulations resulting from the use of Equations (3.2-1) through (3.2-57) for the CSM and Soyuz fine tone loops are given in Table 3-2. This data should replace similar information contained in Reference 1. The Apollo design values, to which the data has been fitted are enclosed in boxes; the ASTP and Apollo systems are assumed to have the same characteristics for a given value of received power. Note that the range entries are included for reference only and do not represent parametric data, since received power is the independent parameter to which range is related through Equation (3.2-1). This fact requires separate range entries for Apollo and ASTP, since the specified circuit losses, antenna gains, etc. are not the same for the two systems.

3.2.5 Mid and Coarse Tone Tracking Loop Considerations

During acquisition, when the mid and coarse ranging tones are being transmitted, Equation (3.2-32) gives the CSM IF SNR in the presence of noise transmitted from the Soyuz. This formula accounts for the fact that the net transmitted signal power is reduced by the transmitted noise power, the total transmitted power being constant.

If the tracking loops operate on the effective received signal component*, rather than on the total received power as assumed in paragraph 3.2.4, Equation (3.2-47), is not sufficient for computing the mid and coarse loop gains. A correction is required that reduces the total received power to reflect the net received signal power. The

*A similar discussion is presented in paragraph 3.3.1.

Table 3-2. VHF RANGING SYSTEM FINE LOOP PARAMETERS[1]

RANGE[1] APOLLO (km)	APOLLO (n.mi.)	ASTP (km)	ASTP (n.mi.)	P_R(dBm)[2] (Avg.Modulated) CSM	P_R(dBm)[2] (Avg.Modulated) LM/SOYUZ	K_L CSM	K_L LM/SOYUZ	$2B_L$ (Hz) CSM	$2B_L$ (Hz) LM/SOYUZ	$(2B_L)_{LC}$ / $(2B_L)_{SC}$ (Hz)	ω_n (rad/sec) CSM	ω_n (rad/sec) LM/SOYUZ	ζ CSM	ζ LM/SOYUZ
		740.8	400	-117.6	-116.4	2.112	181.7	0.8204	25.06	0.5849	0.6256	8.838	0.2859	0.2698
740.8	400			-116.0	-114.9	3.998	343.9	1.053	27.24	0.8179	0.8608	12.16	0.2972	0.3555
		370.4	200	-111.6	-110.4	14.54	1250	1.700	37.38	1.469	1.641	23.19	0.4180	0.6533
370.4	200			-110.0	-108.8	20.00	1720	1.950	43.20	1.722	1.925	27.20	0.4722	0.7633
		185.2	100	-105.5	-104.4	38.13	3280	2.715	60.95	2.499	2.658	37.55	0.6204	1.049
185.2	100			-104.0	-102.8	44.73	3847	2.984	67.40	2.772	2.879	40.67	0.6663	1.135
		92.6	50	-99.53	-98.37	61.77	5312	3.672	84.05	3.468	3.383	47.79	0.7726	1.332
92.6	50			-97.96	-96.80	66.89	5753	3.878	89.06	3.676	3.521	49.74	0.8018	1.386
		0.09	0.05	-39.53	-38.37	99.99	8599	5.200	121.4	5.009	4.304	60.81	0.9696	1.693
0.09	0.05			-37.96	-36.80	100.0	8600	5.200	121.4	5.009	4.305	60.81	0.9697	1.693

NOTES: 1. Design values to which model is fitted are enclosed in boxes. All other entries are calculated from the fitted model. Range values are included for reference only, being related to received power through the propagation equation.

2. All entries have been calculated from the received power levels shown, where only ranging modulation is assumed to be present in the signal; specifically, no voice modulation is present. Note that ranges differing by factors of 2, as in this table, have corresponding received power levels differing by approximately 6.0206 dB.

required correction is of the form

$$P_{RS} = \left(\frac{SNR_{TS}}{SNR_{TS} + 1} \right) P_R \quad , \qquad (3.2\text{-}58)$$

where

P_{RS} = net received signal power at the CSM (mw)

SNR_{TS} = transmitted SNR from the Soyuz, from Equation (3.2-27), and

P_R = total received power at the CSM, from Equations (3.2-11) or (3.2-14).

The appropriate loop gain formula would thus be

$$K_L = KL1(K1DK2)^{R1DR1M2} \cdot \left(\sqrt{\frac{SNR_{TS}+1}{SNR_{TS}}} \cdot SQPR2X \cdot R - 1 \right) \quad , \qquad (3.2\text{-}59)$$

which would take the place of Equation (3.2-47) for the mid and coarse tone cases. The corresponding loop bandwidths, etc. would be calculated using the normal formulas.

3.2.6 Loop Signal-to-Noise Ratio

The early-late gate model for the CSM fine tone loop signal to noise ratio is

$$SNR_{LC} = 1.916569 \times 10^{-4} K_1 (B_{IFC}/2B_{LC}) SNR_{IFC} \quad , \qquad (3.2\text{-}60)$$

where

K_1 = envelope detector degradation factor (see paragraph 3.2.7)

B_{IFC} = CSM IF equivalent noise bandwidth (two-sided at baseband, has the same value as one-sided at IF; cf. Equation 3.2-17)

$2BLC$ = CSM fine tone two-sided equivalent noise bandwidth, from Equation (3.2-51), and

SNR_{IFC} = CSM IF signal to noise ratio, from Equation (3.2-22).

Since no specific model presently exists for the Soyuz fine tone loop, Equation (3.2-60) is assumed to apply, with suitable substitution of Soyuz parameters.

The CSM mid and coarse tone loop signal to noise ratios are computed without early-late gate degradation:

$$SNR_L = K_1(B_{IFC}/2B_L)\ SNR_{IF}\ , \qquad (3.2\text{-}61)$$

where

SNR_L = CSM mid or coarse loop SNR

K_1 = envelope detector degradation factor, using the Equation (3.2-32) value of SNR_{IF} as input

$2B_L$ = mid or coarse loop bandwidth, from Equation (3.2-51) with loop gain value from Equation (3.2-47), for the total received power assumption, or from Equation (3.2-59), for the received signal power assumption, and

SNR_{IF} = CSM IF SNR, from Equation (3.2-32) .

3.2.7 Envelope Detector Degradation Factor

Envelope detector degradation is modelled using Fubini's universal curve (Reference 9). A piecewise linear model is defined in Table 3-3. To obtain the envelope detector output signal to noise ratio (linear), the normalized output SNR (linear) obtained from the model should be multiplied by the ratio of IF to audio bandwidths. But, as discussed in paragraph 3.2.3, this ratio is assumed to have a value of 1.0, so the modelled envelope detector SNR is the normalized value as shown in the table.

Table 3-3. ENVELOPE DETECTOR DEGRADATION FACTOR

(Piecewise linear approximation of Fubini's universal curve)

INPUT CARRIER OR IF SNR X (dB)	NORMALIZED OUTPUT SNR Y (dB)	DETECTOR DEGRADATION FACTOR K1 (linear)	K1 (dB)	PIECEWISE LINEAR MODEL
>10	(X)	1.0	0	K1(dB) = 0
10	10.0	1.0	0	
9	8.885	0.9739	-0.115	
8	7.77	0.9484	-0.23	K1(dB) = 0.115 X - 1.15
7	6.655	0.9236	-0.345	
6	5.54	0.8995	-0.46	
5	4.39	0.8690	-0.61	
4	3.24	0.8395	-0.76	K1(dB) = 0.15 X - 1.36
3	2.09	0.8110	-0.91	
2	0.94	0.7834	-1.06	
1	-0.2475	0.7503	-1.2475	
0	-1.435	0.7186	-1.435	K1(dB) = 0.1875 X - 1.435
-1	-2.6225	0.6883	-1.6225	
-2	-3.81	0.6592	-1.81	
-3	-5.185	0.6046	-2.185	
-4	-6.56	0.5546	-2.56	K1(dB) = 0.375 X - 1.06
-5	-7.935	0.5087	-2.935	
-6	-9.31	0.4667	-3.31	
-7	-10.81	0.4159	-3.81	
-8	-12.31	0.3707	-4.31	K1(dB) = 0.5 X - 0.31
-9	-13.81	0.3304	-4.81	
-10	-15.31	0.2944	-5.31	
-11	-16.9975	0.2513	-5.9975	
-12	-18.85	0.2145	-6.685	K1(dB) = 0.6875 X + 1.565
-13	-20.3725	0.1831	-7.3725	
-14	-22.06	0.1563	-8.06	
<-14	(5.94-2X)	<0.1563	<-8.06	K1(dB) = X + 5.94

Y = X + K1(dB); Actual Y(linear) = Normalized Y(linear) $\cdot(B_{IF}/2B_{Audio})$

3.2.8 Unlock Factors

Once the ranging acquisition sequence has been completed, the Soyuz fine tone loop, having the wider bandwidth, will determine when the system loses lock. If unlock is defined as the skipping of one or more cycles of the received ranging tone, the average time to unlock can be defined as the average elapsed time to skip one cycle

$$T_{av} = \frac{2}{\omega_{ns}} e^{\pi \, SNR_{LS}} \qquad (3.2\text{-}62)$$

where

ω_{ns} = Soyuz fine tone loop natural resonant frequency (rad/sec), from Equation (3.2-54), and

SNR_{LS} = Soyuz fine tone loop signal to noise ratio, from the Soyuz equivalent of Equation (3.2-60).

The unlock probability is defined as the probability that a cycle has been skipped within elapsed time T(sec)

$$P_{UNLOCK}\ (t \leq T) = 1 - e^{-T/T_{av}} \quad . \qquad (3.2\text{-}63)$$

In a manner analogous to reliability computations, where the probability of a failure increases with elapsed time, the probability of unlock increases as the total time over which range tracking is required increases.

The values of T used in Equation (3.2-63) should represent the expected duration of the tracking periods during rendezvous. Table VIII of Reference 10 lists two VHF tracking periods: 20 minutes prior to the CSM NSR maneuver (49:31 to 49:51 hr:min Soyuz g.e.t.) and 16 minutes after the CSM TPI maneuver (51:04 to 51:20). A third tracking period which is listed as being only sextant tracking but also might involve VHF tracking is 34 minutes prior to TPI (50:08 to 50:42). The entire

time intervals between the beginning of VHF tracking and NSR is 31 minutes (49:31 to 50:02), the period between NSR and TPI is 56 minutes (50:02 to 50:08), and the period from TPI to final breaking is 32 minutes (50:58 to 51:30). If Equation (3.2-63) is evaluated using values of T, for example, of 10, 20, 30, 40, 50, and 60 minutes (600 to 3600 seconds), a family of parametric curves versus received power (or range) can be obtained.

3.2.9 Range Error Factors

Range error consists of a bias offset due to the relative range-rate between the vehicles (the tracking loops must operate with non-zero steady-state errors to match the incoming doppler shift), plus random errors due to thermal noise (loop jitter), oscillator instability, readout granularity, system phase delay variations, and interference between the voice and ranging signals (when used simultaneously). The range error due to range-rate (velocity error) can be considered as the mean or expected value of the range error random variable, while the root-sum-square (RSS) of the rms values of the other errors can be considered as the 1σ limit of the random process. This treatment assumes that the other errors are functionally independent and that it is meaningful to add their variances to obtain the net variance.

The range error bias or offset due to range-rate (steady-state velocity error) is

$$\Delta R_{RR} = RR/K_{LC} \ , \qquad (3.2\text{-}64)$$

where

ΔR_{RR} = range error offset (meters)

RR = steady-state relative range-rate between the vehicles (meters/sec), and

K_{LC} = CSM fine tone loop gain, from Equation (3.2-47).

For the purposes of the model implementation, instantaneous relative rate-of-change of range rate (acceleration) is assumed to be negligible, so that only "constant" velocity considerations apply. At the present time, very little data is available regarding the expected variation of range-rate with range for the ASTP rendezvous. Table I of Reference 10 lists the final breaking gates (from about 2 km range to station keeping), and Table VIII of the reference lists times and ranges for specific mission events. Computing average range-rates from this data, and assuming equivalent straight line variations between the CSM burn events, the range-rate versus range model shown in Figure 3-1 and Table 3-3 can be obtained.

The assumed functional form of the range-rate model is

$$RR = m_i R_{KM} + b_i \quad , \tag{3.2-65}$$

where

RR = range-rate (meters/sec)

i = model segment number (as noted in the figure and table), and

R_{KM} = vehicle-to-vehicle range (km).

The values for m_i and b_i can be calculated from

$$m_i = (RR_i - RR_j)/(R_{KMi} - R_{KMj}) \tag{3.2-66}$$

$$b_i = RR_i - m_i R_{KMi} \quad ,$$

where

RR_i = range-rate value from the table at the end of model segment i.

RR_j = range-rate at the beginning of segment i ($RR_i > RR_j$)

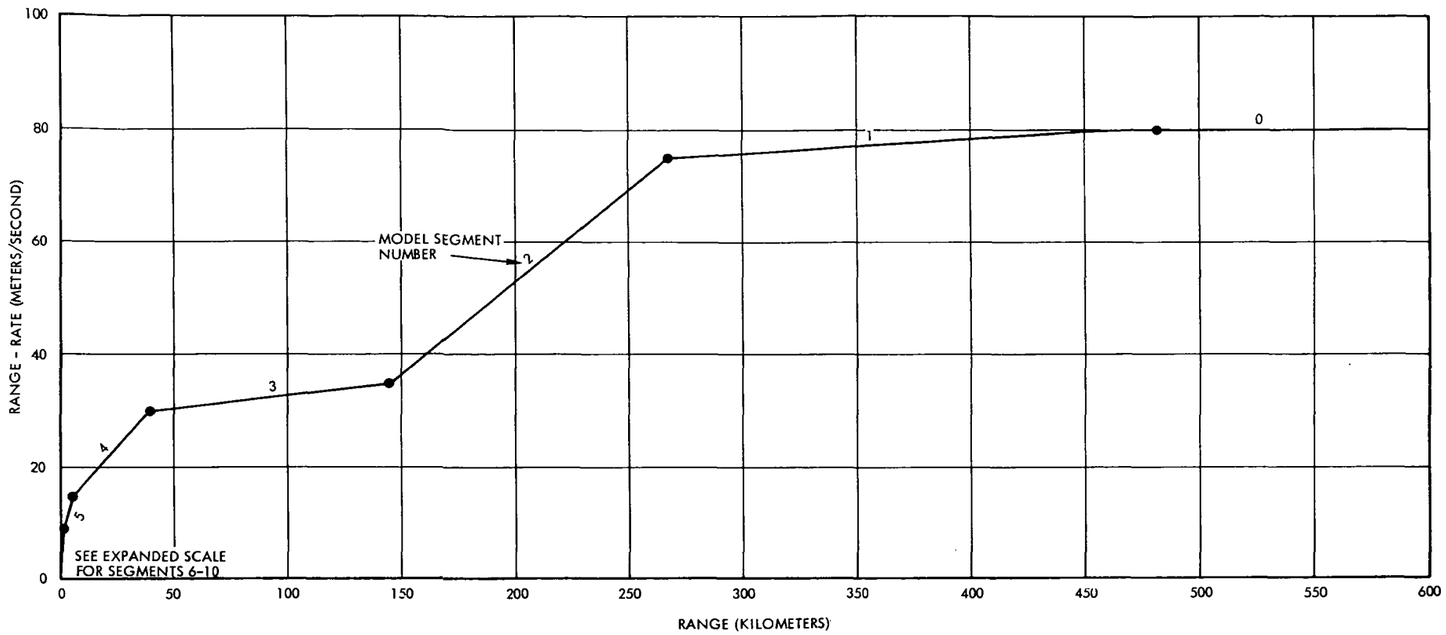

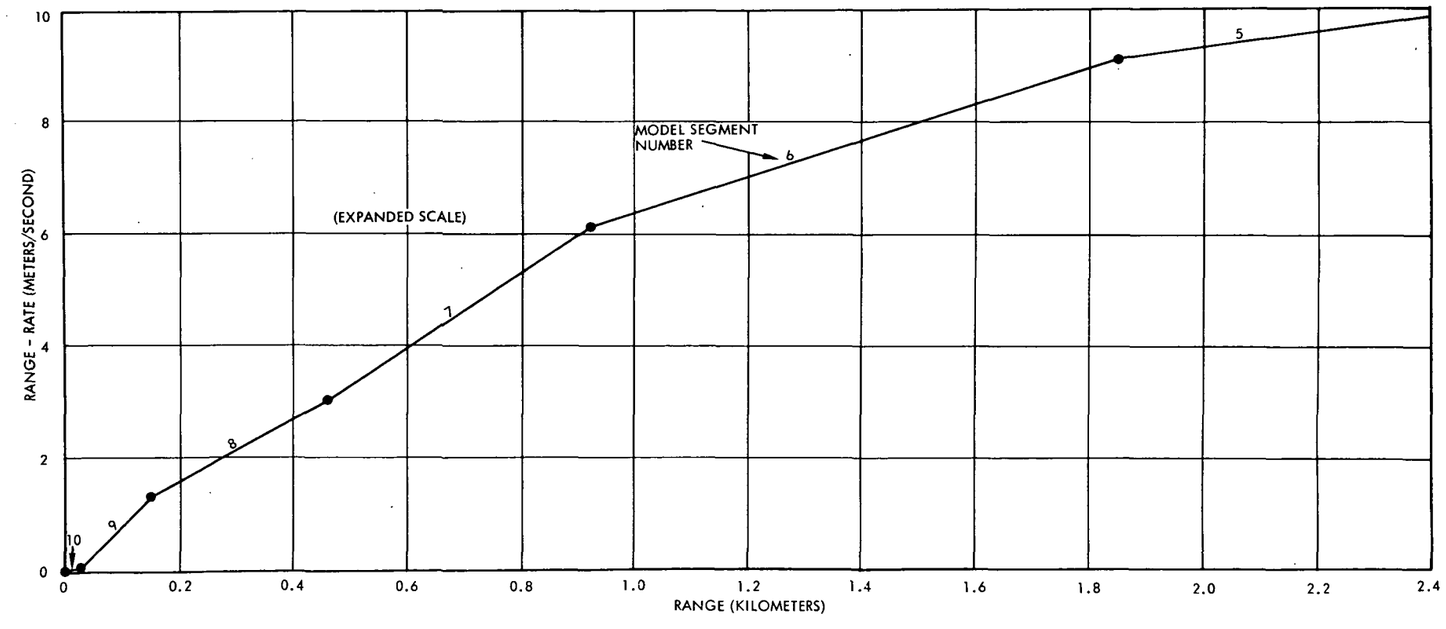

Figure 3-1. Range-Rate Versus Range Model

Table 3-4. BREAKPOINTS FOR RANGE-RATE VERSUS RANGE MODEL

RANGE (km)	RANGE-RATE (meters/sec)	MODEL SEGMENT NUMBER	CSM BURN EVENT (where applicable)
>478.0	80	0	NC2
478.0	80	1	NCC
267.6	75	2	NSR
146.7	35	3	TPI
39.6	30	4	
6.0	15	5	
1.85	9.1	6	
0.925	6.1	7	
0.46	3.0	8	
0.15	1.5	9	
0.03	0.03	10	
0	0		

R_{KMi} = range value from the table at the end of model segment i, and

R_{KMj} = range at the beginning of segment i ($R_{KMi} > R_{KMj}$).

The values of these coefficients have not been precalculated pending a better specification of range-rate versus range.

The rms range error at the CSM due to system thermal noise is

$$\sigma_{RS} = \frac{c}{2\omega_t}\sqrt{\frac{1 + (T_S/T_C)(B_{SC}/B_C)}{2\ SNR_{LC}}}\ , \qquad (3.2\text{-}68)$$

where

σ_{RS} = rms error (meters)

c = velocity of light in a vacuum, (2.997925×10^8 meters/sec)

ω_t = fine ranging tone frequency ($2\pi \cdot 31.6 \times 10^3$ rad/sec)

T_S, T_C = system noise temperatures as in Equation (3.2-16)

B_{SC} = Soyuz and CSM cascaded loop bandwidth (two-sided)

B_C = CSM loop bandwidth (two-sided) from Equation (3.2-51), and

SNR_{LC} = CSM loop SNR, from Equation (3.2-60).

If K1 represents the Soyuz fine tone loop gain, from Equation (3.2-47), and K2 represents the CSM fine tone loop gain, also from Equation (3.2-47), then Reference 1 gives the cascaded loop bandwidth as

$$B_{SC} = 2B_{LSC} = \frac{\begin{array}{l} K1\ K2\ (1 + 3.89\ K1 + 1.27\ K2 \\ + 0.244\ K1\ K2 + 0.213\ K1^2 + 0.366\ K2^2 \\ + 0.00868\ K1^2\ K2 + 0.0294\ K1\ K2^2 \\ + 3.83 \times 10^{-5}\ K1^2\ K2^2) \end{array}}{\begin{array}{l} 2(K1 + K2 + 3.89\ K1^2 + 1.27\ K2^2 - 2.06\ K1\ K2 \\ + 0.213\ K1^3 + 0.366\ K2^3 + 1.6\ K1^2\ K2 \\ - 0.986\ K1\ K2^2 + 0.317\ K1^2\ K2^2 \\ + 0.095\ K1^3\ K2 + 0.05\ K1\ K2^3 \\ + 0.0047\ K1^3\ K2^2 + 0.00161\ K1^2\ K2^3) \end{array}} \qquad (3.2\text{-}69)$$

Completing the range error model, the rms range error due to oscillator instability is

$$\sigma_{RO} = 10^{-6}\ R\ , \qquad (3.2\text{-}70)$$

the rms range error due to readout granularity is

$$\sigma_{RG} = 5.3553614 \text{ meters}\ , \qquad (3.2\text{-}71)$$

and the rms range error due to phase delay variations is

$$\sigma_{RP} = 14.989625 \text{ meters}\ . \qquad (3.2\text{-}72)$$

The rms range error due to simultaneous voice and ranging interference requires separate treatment and is discussed in paragraph 3.3.2.

The total range error model for ranging only operation is

$$\varepsilon_R = \Delta R_{RR} \pm \sqrt{\sigma_{RS}^2 + \sigma_{RO}^2 + \sigma_{RG}^2 + \sigma_{RP}^2}\ , \qquad (3.2\text{-}73)$$

where ΔR_{RR} represents the average or expected value of the range error, and ε_R provides the 1σ limits of the range error.

3.2.10 Probability of Correct Range Measurement

The form of Equation (3.2-73) shows that there will always be an error in the range measurement unless, as shown by Equation (3.2-64), the relative range-rate is zero. In this case, ΔR_{RR} is zero, and Equation (3.2-73) yields the 1σ limit of the random error process. If the random errors were assumed to be gaussian, then the standard statements regarding the probabilities that the range error is less than 1σ, 2σ, 3σ, etc. could be applied. If the random errors were assumed to have unkown statistics, then the Chebyshev or Chernoff bounds could be applied.

However, since the range-rate model being proposed has zero range-rate only at zero range, the concept of correct range measurement seems academic, since Equation (3.2-73) shows that there will always be some error in the measurement. A more appropriate probability concept would appear to be that implied directly by Equation (3.2-73), namely that the 1σ limits of the range error are as defined, from which probability statements can be made regarding the limits over which the range error can be expected to vary.

3.2.11 Acquisition Time Factors

Defining acquisition time in terms of Figure D.2-8 from Appendix D,

$$T_{acq_L} = K_{TA}/2B_L \ , \qquad (3.2\text{-}74)$$

where

T_{acq_L} = expected acquisition time (sec) for each of the tracking loops

K_{TA} = acquisition time model factor, and

$2B_L$ = two-sided loop bandwidth of loop for which acquisition time is being calculated, from Equation (3.2-51).

The piecewise linear model for the K_{TA} factor is

$$K_{TA} = a\ SNR_{LdB} + b\ , \tag{3.2-75}$$

where

SNR_{LdB} = loop SNR (in dB) whose linear value is obtained from Equation (3.2-60) or (3.2-61), as appropriate to the loop being considered.

Implementing Figure D.2-8 from Appendix D,

$$K_{TA} = \begin{cases} 2.0 & , SNR_{LdB} \geq 21.5 \text{ dB} \\ -0.16842105\ SNR_{LdB} + 5.6210526, & 12 \text{ dB} \leq SNR_{LdB} \leq 21.5 \text{ dB} \\ -0.88421053\ SNR_{LdB} + 14.210526\ , & SNR_{LdB} \leq 12 \text{ dB}. \end{cases} \tag{3.2-76}$$

Equation (3.2-74) gives the expected loop acquisition time (sec) for each loop, so the expected total acquisition time is

$$T_{acq} = T_{acq_{\substack{CSM \\ mid}}} + T_{acq_{\substack{CSM \\ coarse}}} + T_{acq_{\substack{Soyuz \\ fine}}} + T_{acq_{\substack{CSM \\ fine}}}\ . \tag{3.2-77}$$

3.3 SIMULTANEOUS VOICE AND RANGING IMPLEMENTATION

The subject of simultaneous transmission of voice and ranging signals complicates the math model as presented previously, because the transmitted power is reduced, the available signal power is further reduced, and there is intermodulation interference between the voice and ranging signals. The following paragraphs develop the correction factors to be applied to the previous formulas, when the case of simultaneous voice and ranging is considered.

3.3.1 Transmitted and Received Power

In the case of ranging signals alone, the transmitted signal is of the form

$$s(t) = aR(t) \cos \omega_c t \ , \tag{3.3-1}$$

where

a = peak signal amplitude (volts)

$R(t)$ = 0 or 1 = ranging tone square wave, and

ω_c = RF carrier frequency (rad/sec) ,

the peak (unmodulated) transmit power is

$$P_{T_{peak}} = \frac{a^2}{2} \ , \tag{3.3-2}$$

and the average modulated transmit power is

$$P_{T_{av}} = \frac{a^2}{4} \ . \tag{3.3-3}$$

Expressing the ranging tone modulation as

$$R(t) = \frac{1}{2} + \frac{1}{2} SQ_R(t) \ , \tag{3.3-4}$$

where

$$SQ_R(t) = \pm 1 \text{ square wave,}$$

Equation (3.3-1) can be rewritten as

$$\begin{aligned} s(t) &= a \left[\frac{1}{2} + \frac{1}{2} SQ_R(t) \right] \cos \omega_c t \\ &= \frac{a}{2} \cos \omega_c t + \frac{a}{2} SQ_R(t) \cos \omega_c t, \end{aligned} \tag{3.3-5}$$

from which the carrier power and ranging sideband power can be seen to be equal and given by

$$P_C = P_{RS} = \frac{a^2}{8} \ . \tag{3.3-6}$$

When voice is transmitted simultaneously with ranging, the transmitted signal is of the form

$$s(t) = a\, R(t)\, V(t) \cos \omega_c t \ , \tag{3.3-7}$$

where

$$V(t) = \frac{1}{2} + \frac{1}{2} SQ_V(t) = \text{equivalent voice square wave.}$$

Following the approach leading up to Equation (3.3-5),

$$\begin{aligned} s(t) &= a \left[\frac{1}{2} + \frac{1}{2} SQ_R(t) \right] \left[\frac{1}{2} + \frac{1}{2} SQ_V(t) \right] \cos \omega_c t \\ &= \frac{a}{4} \cos \omega_c t + \frac{a}{4} SQ_R(t) \cos \omega_c t + \frac{a}{4} SQ_V(t) \cos \omega_c t \\ &\quad + \frac{a}{4} SQ_R(t)\, SQ_V(t) \cos \omega_c t \ , \end{aligned} \tag{3.3-8}$$

from which the average modulated transmit power can be seen to be

$$P_{T_{av}} = \frac{a^2}{8} \ , \tag{3.3-9}$$

and the carrier power, ranging sideband power, voice sideband power, and cross modulation sideband power can be seen to be equal and given by

$$P_C = P_{RS} = P_{VS} = P_{XS} = \frac{a^2}{32} \ . \tag{3.3-10}$$

Note that the average modulated power is half that for ranging alone, and that the ranging sideband power is one-fourth its original value.*

*Similar comments would apply if one were comparing voice only with simultaneous voice and ranging.

Assuming that the ranging system "recognizes" only signals of the form in Equation (3.3-5), all but the first two terms in Equation (3.3-8) can be considered as noise and interference to the ranging trackers. The net useful ranging signal thus has one-fourth its original power. The formulas presented previously can be used for voice plus ranging if the total received power is multiplied by 0.25 or, equivalently, if the range loss factor is multiplied by 0.25 or the range is multiplied by 2.*

Note, however, that the loop gain data presented in paragraph 3.2.4 shows that the loop gain is reduced by half when the total received power is reduced by half due to the simultaneous voice and ranging modulation. For this fact to be compatible with Equations (3.3-8) and (3.3-5), loop gain must be assumed to be a function of received ranging signal amplitude rather than power as implied in the previous paragraph. This is a comfortable assumption in light of the fact that the loop gain of conventional second-order phase lock loops is proportional to signal amplitude. The resultant correction factors for the loop gain formulas would then be 0.5 for the total received power (or range loss) and $\sqrt{2}$ for the range. The loop signal-to-noise ratio would still require the correction factors assumed in the previous paragraph.**

Trial substitutions of these latest assumptions regarding loop gain for simultaneous voice and ranging into Equation (3.2-47) lead to some interesting results. The design range R2 = 200 n. mi. for the Apollo data becomes about 283 n. mi. ($\sqrt{2}$ 200), which yield a CSM fine tone loop gain of 10 and a LM fine tone loop gain of 860, which are precisely the desired values. Unfortunately, the design range

---

*The resultant IF SNR would represent ranging signal-to-noise ratio, rather than total SNR in this case.

**In Equation (3.2-22), the IF SNR (total signal-to-noise ratio) would be half that obtained for the ranging only case, and Equation (3.2-60) would contain an additional factor of 0.5, for a net loop SNR that is one-fourth that obtained for ranging only.

R1 = 0.05 n. mi., which becomes about 0.071 n. mi., yields a CSM loop gain of slightly less than 100 and a LM loop gain that is slightly less than 8600, which are not half as much as desired. A possible explanation for this discrepancy is that, for simultaneous voice and ranging, the receiver AGC still operates on the total received signal, while the loop is operating only on the ranging component, so that the assumed functional relationship between loop gain and range in Equation (3.2-33) no longer applies. A quick modeling resolution of this discrepancy would be to modify Equation (3.2-47) by adding a multiplicative factor of 0.5 to the calculated loop gain value, instead of incorporating $\sqrt{2}$ R in place of R in the exponent.* Such a modification of Equation (3.2-47) would yield loop gain values that are always half of those obtained for ranging only, but this still may not provide a reasonable functional variation with range. As noted previously, additional loop gain data between the design values used would be required to verify the loop gain models for ranging only and voice plus ranging.

3.3.2 Range Error Considerations

In addition to the range errors discussed in paragraph 3.2.9, the simultaneous voice and ranging model must include the effect of intermodulation (IM) interference between the voice and ranging signals. The IM effects to be accounted for can be considered as being generated by the fourth term in Equation (3.3-8), which shows the product of the two modulating square waves. The model for the rms range error due to intermodulation between the voice and ranging signals (voice transmission from Soyuz to CSM only) is

*Separate loop bandwidth calculation corrections of the form of Equation (3.2-51) may be required for simultaneous voice and ranging, to fit the design values given for loop bandwidth.

$$\sigma_{RI} = \frac{c}{2\omega_t \sqrt{2\ SNR_{LI}}} , \qquad (3.3\text{-}11)$$

(cf. equation 3.2-68), where

SNR_{LI} = Additional CSM fine tone loop SNR due to IM of voice and ranging signals.

From Reference 11, the normalized two-sided spectral density of the third-order IM (in the CSM loop) is

$$\phi_{IM}/2 = \frac{42}{2(128)(2.7 \times 10^3)} \text{ watts/Hz} , \qquad (3.3\text{-}12)$$

so the normalized IM "noise" power in the loop is

$$P_{N_{IM}} = \frac{\phi_{IM}}{2} \cdot 2B_L , \qquad (3.3\text{-}13)$$

where

$2B_L$ = CSM fine tone two-sided loop bandwidth, from the simultaneous voice and ranging equivalent of Equation (3.2-51).

Since the normalized ranging signal power in the loop is 0.5 watts, the loop SNR due solely to IM of voice and signal is

$$SNR_{LI} = \frac{1/2}{(\phi_{IM}/2)(2B_L)} = \frac{2(128)(2.7 \times 10^3)}{2(42)(2B_L)}$$

$$= 8228.5714/2B_L , \qquad (3.3\text{-}14)$$

and Equation (3.3-11) becomes

$$\sigma_{RI} = \frac{c}{2\omega_t \sqrt{2(8228.5714)/2B_L}}$$

$$= \frac{c}{2\omega_t} (0.0077951196)\sqrt{2B_L} . \qquad (3.3\text{-}15)$$

The total range error model for the voice plus ranging case is (cf. Equation 3.2-73)

$$\epsilon_R = \Delta R_{RR} \pm \sqrt{\sigma_{RS}^2 + \sigma_{RO}^2 + \sigma_{RO}^2 + \sigma_{RP}^3 + \sigma_{RI}^2}\,, \qquad (3.3\text{-}16)$$

where voice plus ranging computations are employed in evaluating ΔR_{RR}, σ_{RS}, and σ_{RI}.

4. MATH MODEL VALIDATION

The mathematical model as described herein has been validated to a limited extent by comparing computer computations with data obtained primarily from previous reports. Calculations of important parameters as accomplished by the model are well within reasonable tolerances when compared to data from other sources. However, the scarcity of test data for validation use is primarily a result of the loss of records due to the length of time which has elapsed between the time of this report and initial system testing (performed in 1967 and 1968). At this time it may not be cost effective to regenerate test data which is required to completely validate the math model.

5. SUMMARY AND CONCLUSIONS

Approximately 6 months of study have been devoted to the development of a mathematical model to be used as a basis for the analysis of the ASTP VHF ranging system performance. A mathematical model of the ranging system has been developed which is based largely on the works of Chang (Reference 1), Eisenhauer and Ridge (Reference 2), RCA (References 3 and 4), Stiffler (Reference 5), and Goldman (Reference 6).

Several of the models chosen and methods for analyses were selected because of their simplicity and accuracy, although several other modelling techniques could have been used effectively.

The model presented in this report will allow the prediction of range error, system acquisition time, probability of unlock, and many other important VHF ranging performance characteristics.

References

1. Chang, C. Y., "VHF Ranging Error Analysis," TRW Interoffice Correspondence (IOC) No. 68:7251-CC-125, 1 November 1968.

2. Eisenhauer, D. R. and L. K. Ridge, "Signal-to-Noise Ratio Analysis of the Fine Tone Tracking Loop of the VHF Ranging System," TRW IOC No. 72:7153.6-88, 13 October 1972.

3. "Apollo VHF Ranging Critical Design Review, Volume II CM VHF/DRG," RCA Defense Communications System Division, Document No. RMM-CDR-1, 28 February to 1 March 1968.

4. "Apollo VHF Ranging Critical Design Review, Volume III LM VHF/RTTA," RCA Defense Communications System Division, Document No. RMM-CDR-1, 28 February to 1 March 1968.

5. Stiffler, J. J., Theory of Synchronous Communications, Prentice-Hall, 1971.

6. Goldman, S. L., "Second-Order Phase-Lock-Loop Acquisition Time in the Presence of Narrow-Band Gaussian Noise," IEEE Transactions on Communications, April 1973.

7. "Circuit Margins for the Radio Communications and Ranging System," ASTP Document IED 50107, 30 June 1973.

8. Ellis, M. R., "Apollo Mission H1 Spacecraft-to-Spacecraft VHF Coverage," TRW Technical Report No. 11176-H375-RO-00, 22 October 1969.

9. Fubini, E. G., "Signal-to-Noise Ratio in AM Receivers," Proceedings of the IRE, December 1948.

10. "Trajectory Plan," ASTP Document ASTP 40200.1, 27 March 1973.

11. Warren, W. B., "Bimonthly Technical Report Number 2, Volume II," TRW Technical Report No. 11176-H042-RO-00, 1 October 1968.

APPENDIX A

ASTP VHF Ranging System - Early/Late Gate Math Model

APPENDIX A

ASTP VHF RANGING SYSTEM - EARLY/LATE GATE MATH MODEL

A.1 INTRODUCTION

A mathematical model is developed in this appendix which may be used in computer analyses of the performance of the Apollo VHF Ranging System as modified for use in the Apollo-Soyuz Test Project (ASTP).

This appendix describes the overall operation of the VHF Ranging System and presents a mathematical model of an Early/Late gate tracking loop based on the works of Chang, Eisenhauer and Ridge.

A.2 DISCUSSION OF OPERATION OF THE VHF RANGING SYSTEM

This section includes a general discussion of the operation of the VHF ranging system and presents the system specifications as given for the Apollo system.

A.2.1 Overall System Operation

The VHF ranging system was added to the existing LM-CSM VHF communications system to provide a backup ranging system for the rendezvous radar. On-off amplitude modulation of the ranging signal on the VHF carrier was chosen as the desired method of ranging signal transmission between the spacecraft. The basic ranging configuration is shown in the sketch of Figure A.1-1. From this sketch it can be seen that both the voice and the ranging signals are applied as on-off amplitude modulation of the VHF carrier. The ranging and voice communication functions can be used simultaneously, except during the acquisition phase of ranging operation. During acquisition, the coarse and mid tone ranging signals are modulated on the VHF carrier. Since these two frequencies lie very close to the audio band, the presence of a voice signal would seriously degrade the performance of the phase locked loops that track the coarse and mid tone ranging signals. The ranging signals would also impair the operation of the voice channel. Consequently, it is an operational requirement of the VHF ranging system that the voice channel must be switched off during the acquisition phase of ranging operation. Once the proper locked condition has been established in the 31.6 kHz fine tone loop, the VHF voice channel is then available for full duplex operation. Because the fine tone ranging frequency of 31.5 kHz lies so far outside the voice frequency band (300 to 3000 Hz), little interference may be expected between voice and ranging signals once fine loop track has been established.

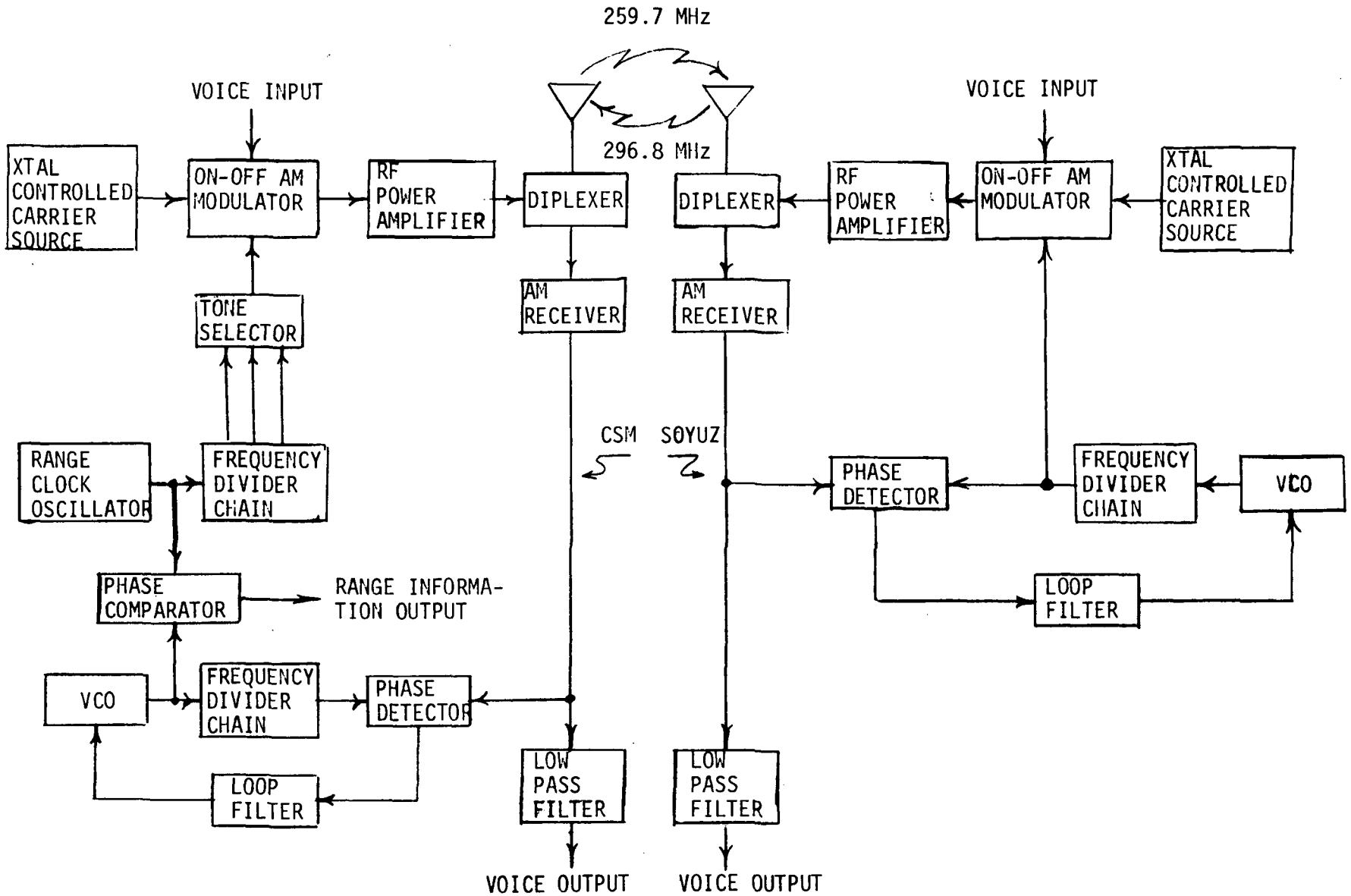

Figure A.1-1. Simplified VHF Ranging System

A.2.2 Functional Description of VHF Ranging

VHF ranging between the Soyuz Spacecraft and the Command Module (CM) is accomplished by on/off keying of a VHF carrier by set tone frequencies. Operating frequencies are:

(a) VHF A-296.8 MHz - this is called the downlink frequency and is transmitted from the Soyuz to CM.

(b) VHF B-259.7 MHz - this is called the uplink signal and is transmitted from CM to Soyuz.

Voice communication can be accomplished during ranging but only when fine tone modulation is present.

A description of the ASTP VHF Ranging System is given in the following sections.

A.2.3 ASTP VHF Ranging System Description (Reference A-1)

The Ranging Tone Transfer Assembly (RTTA), which is located in the Soyuz and operates in conjunction with the Soyuz VHF transceiver, is used as a signal transponder.

The ASTP VHF Ranging System is a three tone system. The ranging signal consists of three square-wave components at 31.6 kHz, 3.95 kHz, and 247 Hz. The 31.6 kHz signal provides the range measurement resolution, while the 3.95 kHz and 247 Hz signals provide unambiguous range measurements for the required 200-n.mi. operating range. A clock drives a tone generator which produces these frequencies. The 3.95 kHz signal is transmitted first; a modulo two combination of 3.95 kHz and 247 Hz is then transmitted. Finally, the 31.6 kHz signal is transmitted to achieve maximum range accuracy. As these signals are selected for transmission, the appropriate tracker servo loop must also be selected in the Command Module to track the signal returned by the Soyuz. In the Soyuz spacecraft, the 31.6 kHz signal is tracked with a VCO loop in order to reconstitute the signal for retransmission. The other ranging signals are merely amplified, clipped and retransmitted. These other frequencies are transmitted during acquisition mode only. An auto-

matic sensor selects which mode is being used in the Soyuz and switches the VCO tracker in and out accordingly.

A description of the operation of each element of the Ranging System follows.

A.2.3.1 The Digital Ranging Generator (DRG)

The Digital Ranging Generator (DRG), located in the CM, in conjunction with the CM VHF Communications transceiver acts in the role of a signal tracker during ranging.

The tracking system operates as follows: Power is initially turned on at the Soyuz and in the Command Module. Power Turn-on resets the program, resets the display in the Command Module, and places the CM data good signal (which indicates to the CM computer when data is available) in the "no-data" condition. The system remains in this null condition until the CM astronaut presses the VHF Ranging Reset switch. This starts the acquisition program. Initially, a 3.95-kHz tone is transmitted; this signal is transponded by the Soyuz, and received and locked by the mid-loop tracker in the Command Module. A 3.95-kHz tone combined with a 247-Hz tone is then transmitted from the CM. This tone is again transponded by the Soyuz, received by the Command Module, and locked by the coarse-loop tracker. This loop locks the 247-Hz signal component and provides for a theoretical unambiguous range readout up to 327 miles. The composite signal is then locked by both the mid-loop tracker and the coarse-loop tracker. This program step provides for finer locking of both the 247-Hz and 3.95-kHz tones components. At this point in the acquisition, a test is conducted to determine if the signal is being tracked properly. If this test fails, a reset occurs and the program returns to a null condition. If, however, the test indicates the track is good, a 31.6-kHz tone is transmitted and 31.6-kHz gating signals gate the CM receiver. The Soyuz has a signal sensor which determines when 3.95-kHz tones are being received; in this period, the Soyuz acts as a simple transponder

However, when the 3.95 kHz tone disappears, the Soyuz attempts to lock the 31.6 kHz signal and gates the Soyuz receiver accordingly. The Soyuz tracks the 31.6-kHz signal receiver, and transmits the tracked signal to the Command Module. The Command Module then tracks the 31.6kHz received, using the fine-loop tracker.

A condition is finally reached whereby the Command Module is tracking the 31.6-kHz signal which it originated and which is delayed by the two-way distance between vehicles. At this point, the following sequence is initiated: the DRG range counter and DRG range register are cleared. The range count is transferred to the DRG range counter. The range count is downcounted to remove equipment delay, and will ultimately read true range. A good-track test is performed to determine whether correct tracking is occurring at this time. If good tracking exists, the range count is ready to be sent to the EMS display. The internal range counter is downcounted to zero at a 31.6-kHz rate. These count pulses are supplied to the EMS display. During this period, range updating also alters the EMS display. The display is now updated and will continue to be updated by the range update pulses generated by the tracker as it tracks the 31.6 kHz tone. At this point, the "data-good" signal is raised to indicate to the CM computer that the computer can call for range readout at any time. The computer sends command readout strobes to the tracker. Upon receipt of the first strobe, the following internal sequence is initiated; the internal range counter and computer output register are cleared. The range is transferred to the DRG range register. A down-count is initiated to remove RF equipment delay. A true range which lies in the range counter is now transferred to the computer output register, a test is then performed to determine if correct tracking has been occuring. (If the test fails, the display is reset, data-good is reset, and the program is returned to a null condition.) If the test passes, the range now lies in the computer output register and is read out by the computer range strobes. Figure A.2-1 is a functional flow of the CM, Figure

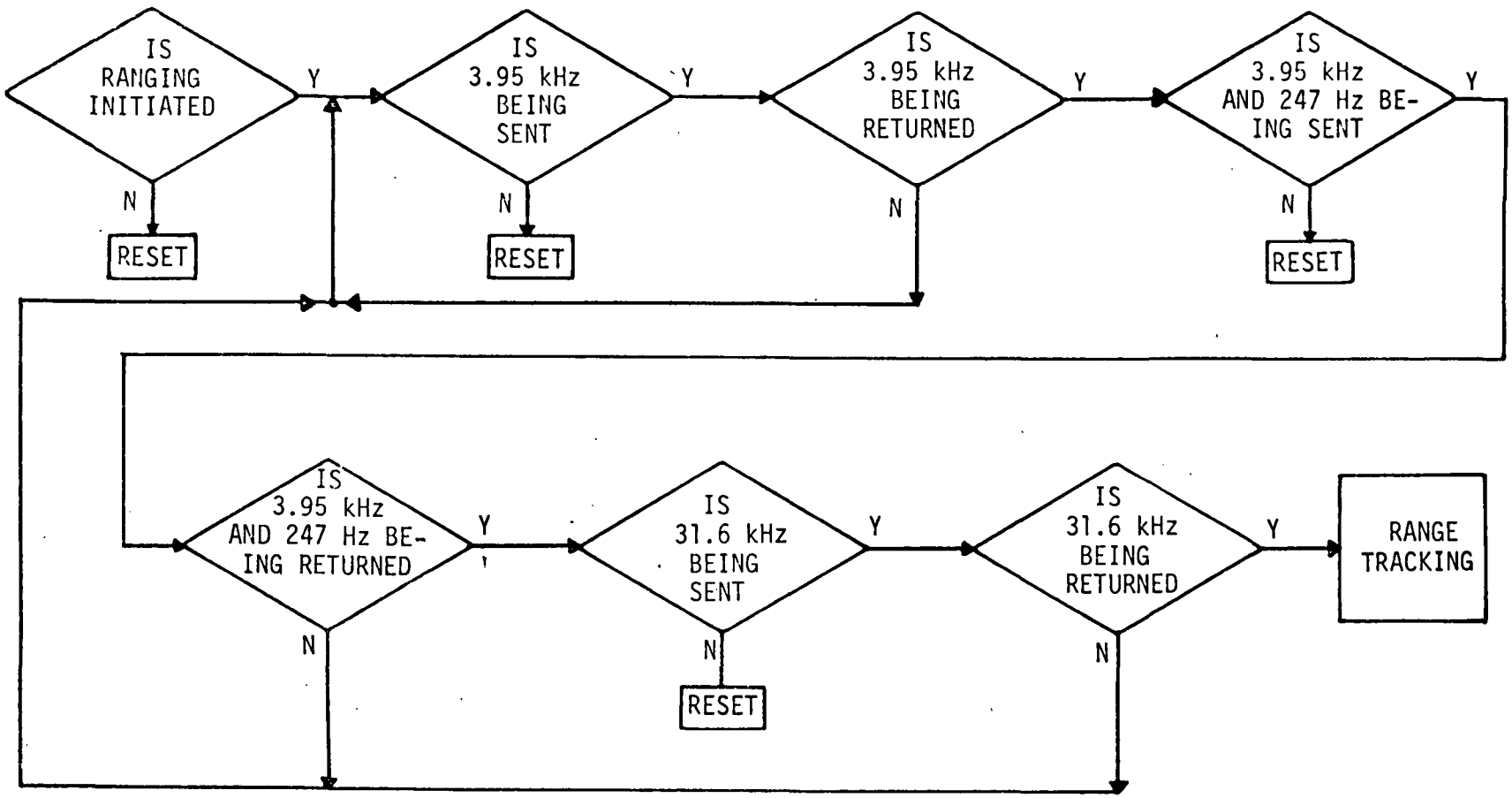

Figure A.2-1. CSM Ranging Acquisition Sequence

A.2-2 is a schematic block diagram of the CM ranging system. Figure A.2-3 is a block diagram of the DRG Tone Generator and Figure A.2-4 is a block diagram of the DRG Tone Tracker.

A.2.3.2 The Ranging Tone Transfer Assembly (RTTA)

The Ranging Tone Transfer Assembly (RTTA), located in the Soyuz, in conjunction with the Soyuz VHF communications transceiver, acts in the role of a signal transponder during ranging. The operation is as follows:

Initially the 3.95-kHz mid-tone is received at the Soyuz. The Soyuz RTTA signal sensor picks up this tone and opens the path for direct retransmission (The received signal is amplified, clipped and retransmitted). The tone next received is the combined 3.95 kHz and 247 Hz tone. This tone which has 247 Hz spectral sidebands centered about 3.95 kHz is accepted by the signal sensor filter. The signal sensor remains activated and direct retransmission continues. Finally the 31.6 kHz tone is received. At this point the signal sensor drops out. Dropout of the signal sensor activates the VCO servo loop. The 31.6-kHz is then tracked. The tracker generates a 31.6-kHz tone phase locked to the received signal and this generated tone is transmitted to the CM. The tracking technique uses an Early/Late 31.6 kHz gating signal. Track is good when the Early and Late signals are altered at a 5.3 kHz rate (three Early, three Late).

These signals gate the RF signal (rather than the audio signal) in order to avoid the large range inaccuracy which would be introduced by the IF delay variations if the audio signal was tracked.

Figure A.2-5 shows the functional flow of the RTTA. Figure A.2-6 is a block diagram of the RTTA.

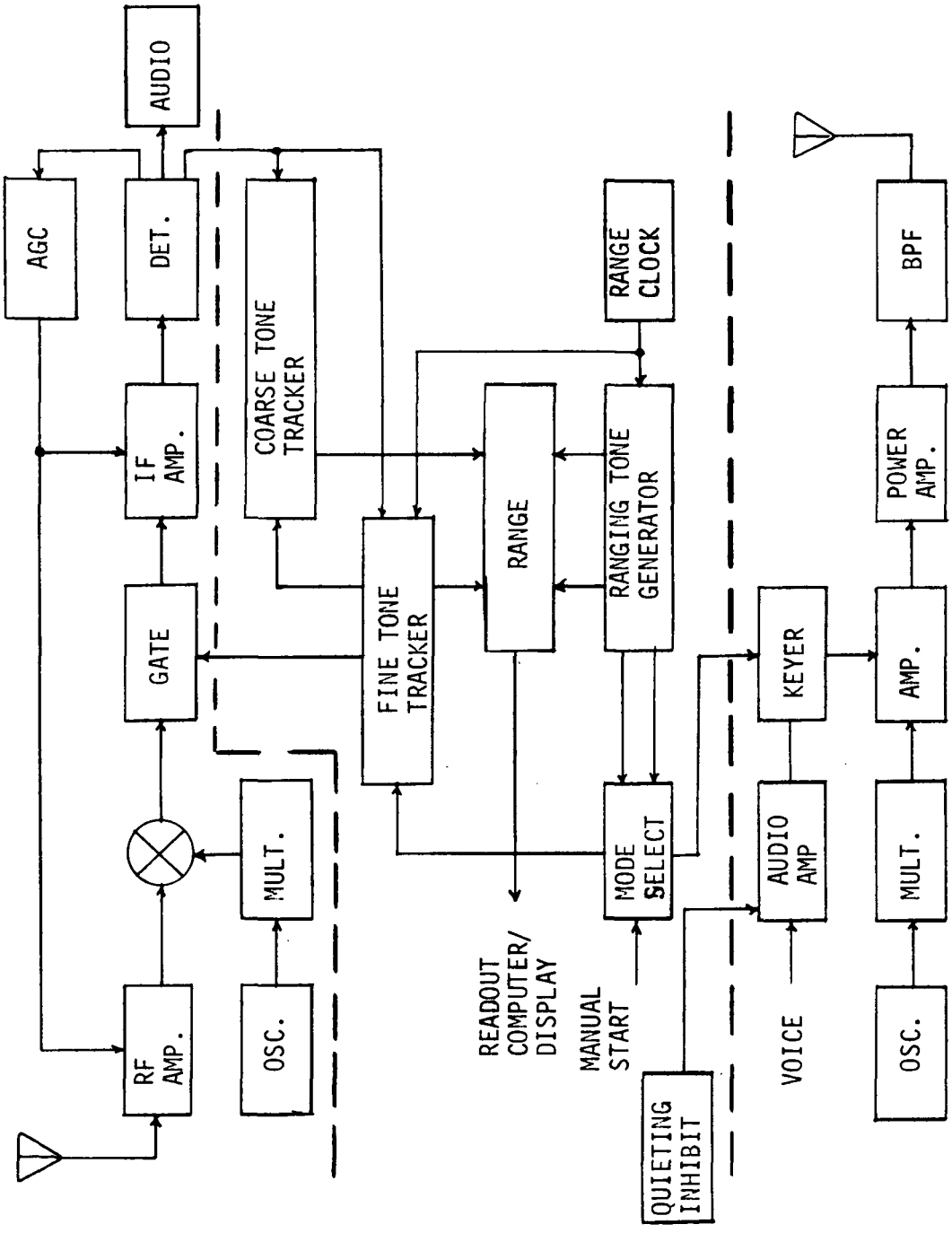

Figure A.2-2. CM Ranging System

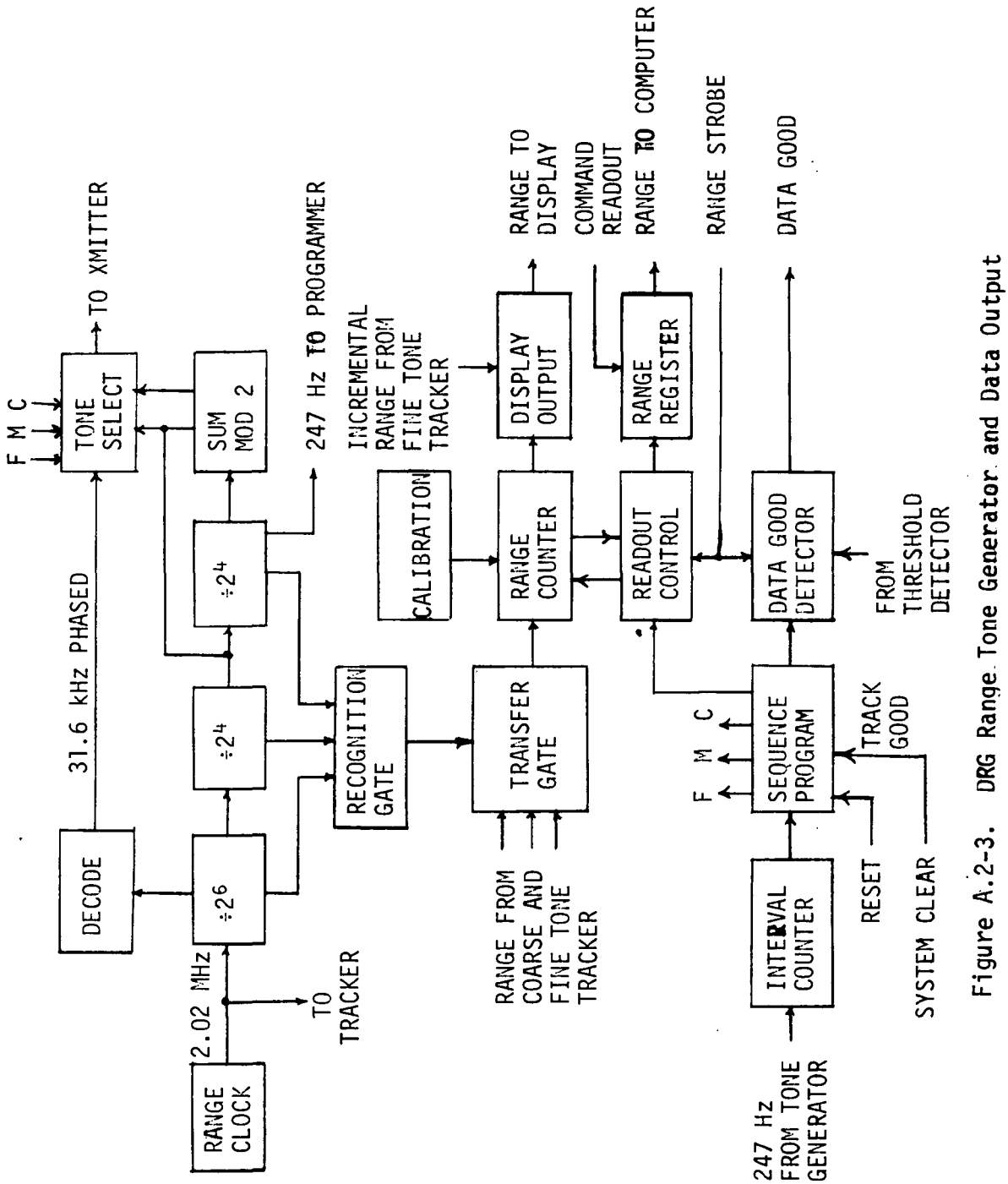

Figure A.2-3. DRG Range Tone Generator and Data Output

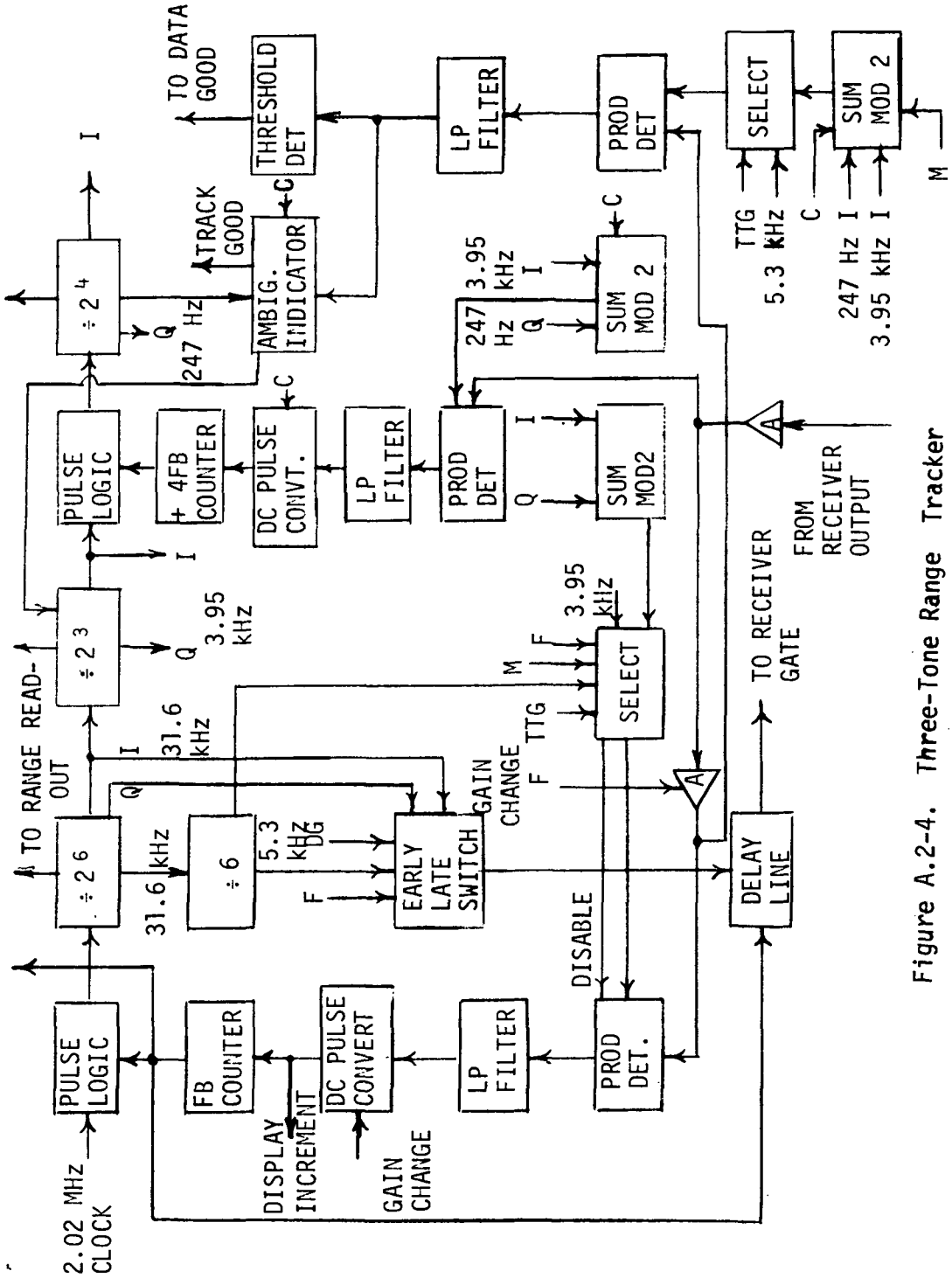

Figure A.2-4. Three-Tone Range Tracker

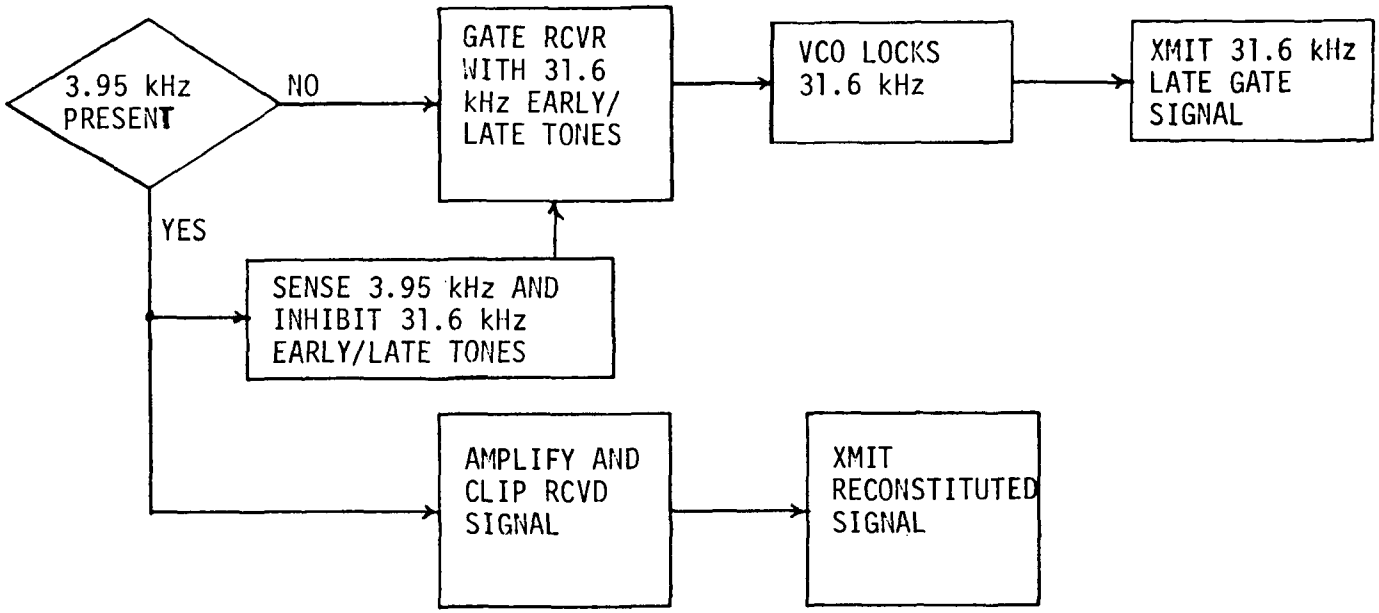

Figure A.2-5. RTTA Functional Flow

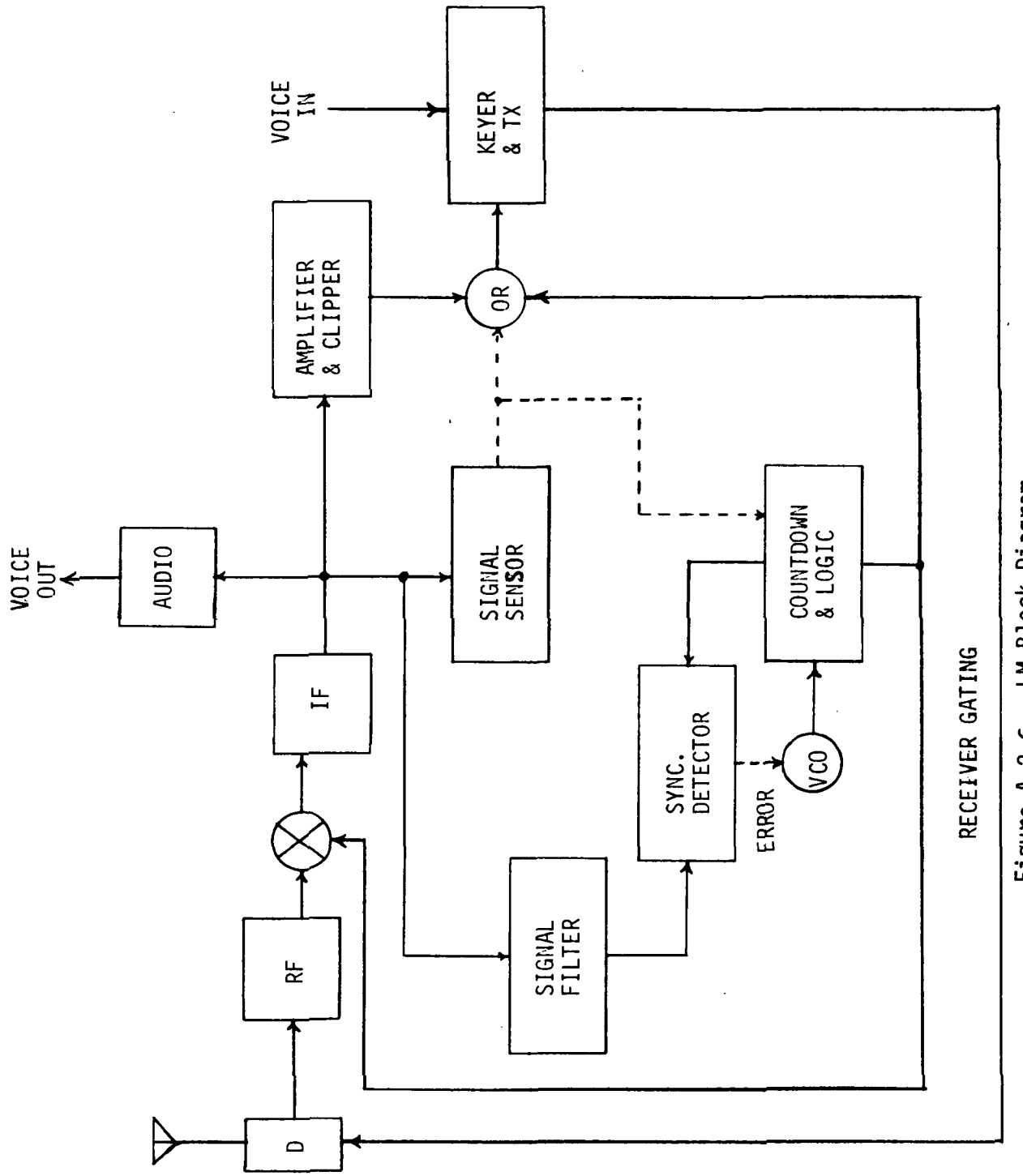

Figure A.2-6. LM Block Diagram

A.2.4 Range Measurement

The range between the Soyuz and CM is measured in terms of the round-trip time delay of the ranging signal. Since the phase shift of the returned ranging signal with respect to the transmitted ranging signal is a linear function of the round-trip time delay, a measurement of this phase shift is a direct measurement of the range. The propagation time, T_p, is given by the fraction of a full cycle of the ranging signal represented by the measured phase shift multiplied by the period of the ranging signal, i.e.,

$$T_p = \frac{\theta_d}{2\pi} \frac{2\pi}{\omega_r} = \frac{\theta_d}{\omega_r} , \qquad \text{(A.2-1)}$$

where

θ_d = the measured phase shift in radians

ω_r = the frequency of the ranging signal

The range corresponding to this propagation time is

$$R = \frac{V_c T_p}{2} = \frac{(3 \times 10^8)}{2} \frac{\theta_d}{\omega_r} = (1.5 \times 10^8) \frac{\theta_d}{\omega_r} \text{ meters} . \qquad \text{(A.2-2)}$$

The range rate can be determined by measuring the change in range as a function of time; i.e., range rate (RR) is

$$RR = \frac{\Delta R}{\Delta t}$$

$$= \frac{1.5 \times 10^8}{\omega_r} \left(\frac{\theta_{d1}}{t_1} - \frac{\theta_{d2}}{t_2} \right) \frac{m}{sec} . \qquad \text{(A.2-3)}$$

Range and range rate of the spacecraft are computed in the CSM on-board computer and are displayed by the EMS.

Since the VHF range measurement is a function of the phase difference between the transmitted and received signals, errors in phase measurement are directly translated to range errors.

A.2.5 EARLY LATE GATE TRACKING LOOP

The phase measurement which provides the basis for the range information is derived by an Early-Late Gate Tracking Loop. A general discussion of the Early Late Gate Loop and an analysis of its operation are given in the following sections.

A.2.5.1 Early/Late Gate Tracking Loop Description

An essential element of the VHF ranging system is a ranging tone phase lock loop (PLL), which is used in both the Command and Service Module (CSM) and Soyuz portions of the ASTP VHF ranging system. In the transponder equipment, which will be used in the Soyuz vehicle, the PLL is used to regenerate a clean ranging tone from the noisy output of the VHF receiver. This clean ranging tone is subsequently amplitude modulated on a VHF carrier which relays the ranging signal back to the CSM. In the CSM, another PLL is used to remove the noise from the ranging tone received from the Soyuz and to supply a clean ranging tone to the CSM range counter. In the normal operation of the ranging system, both the Soyuz and CSM loops are tracking their respective received ranging tones. Since the range between the two vehicles is measured by comparing the phases of the transmitted and received ranging tones in the CSM, the accuracy with which these two loops perform their tracking functions directly influences the accuracy with which the range between the CSM and Soyuz can be measured.

The basic form of the range tone tracking loop is shown in Figure A.2-7. This loop makes use of a somewhat unusual configuration, which employs an "early-late gate" technique to derive a tracking error signal. Some insight into the operation of the loop can be gained from an inspection of Figure A.2-8, which shows typical waveforms existing at various points in the tracking loop.

Waveform A corresponds to the signal coming into the gate at point A. Waveform B is the reference signal for the tracking loop. When the loop is not in "lock", the loop phase error $\delta\phi$ (shown in Figure A.2-8) has a non-zero value. When $\delta\phi$ goes to zero, the pulses of B occur simultaneously with the RF bursts of A. When $\delta\phi$ is non-zero, the early-late gate switching technique generates an error voltage. Waveform C switches on either three early pulses or three late pulses, where the early or late condition means that the pulses have been advanced or retarded by 1/16 cycle (Δ) respectively. Waveform D shows the early-late switched pulses of waveform B. This waveform is multiplied by waveform A in the gate, and waveform E is the resultant. This waveform is amplified, detected, and filtered before passing to the phase detector.

A.2.5.2 Early/Late Gate Tracking Model (High Signal to Noise Ratio)

The phase measurement from which range is derived is obtained by Early-Late Gate Tracking Loop which is generally modelled as a phase locked loop (References A-2 and A-4) as shown in Figure A.2-9.

Gardner (Reference A-4) has shown that the phase error in the output of phase detector of the phase locked loop is

$$\overline{\theta^2}_{no} = \frac{1}{2\left(\frac{S}{N}\right)_{loop}} \qquad (A.2\text{-}4)$$

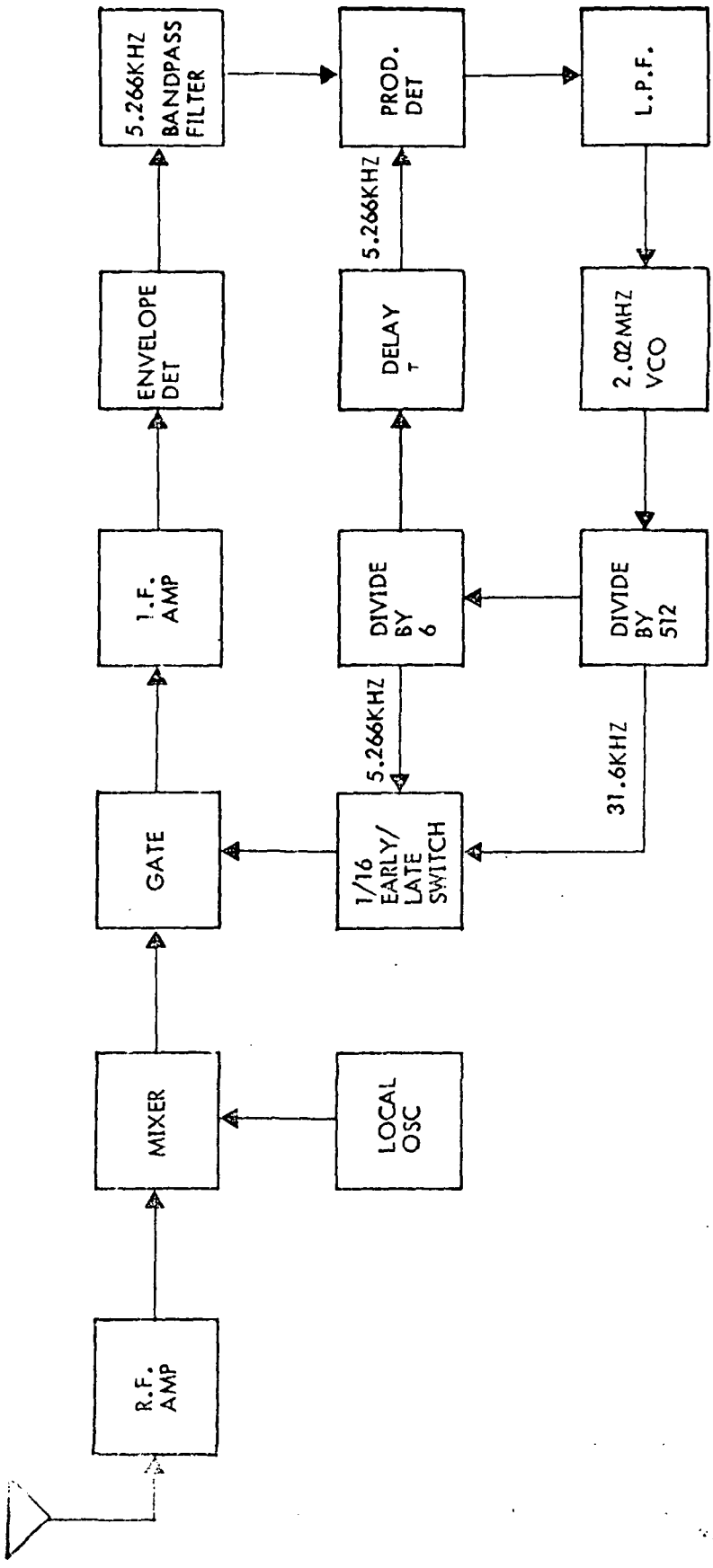

Figure A.2-7. Fine Range Tone Tracker Block Diagram

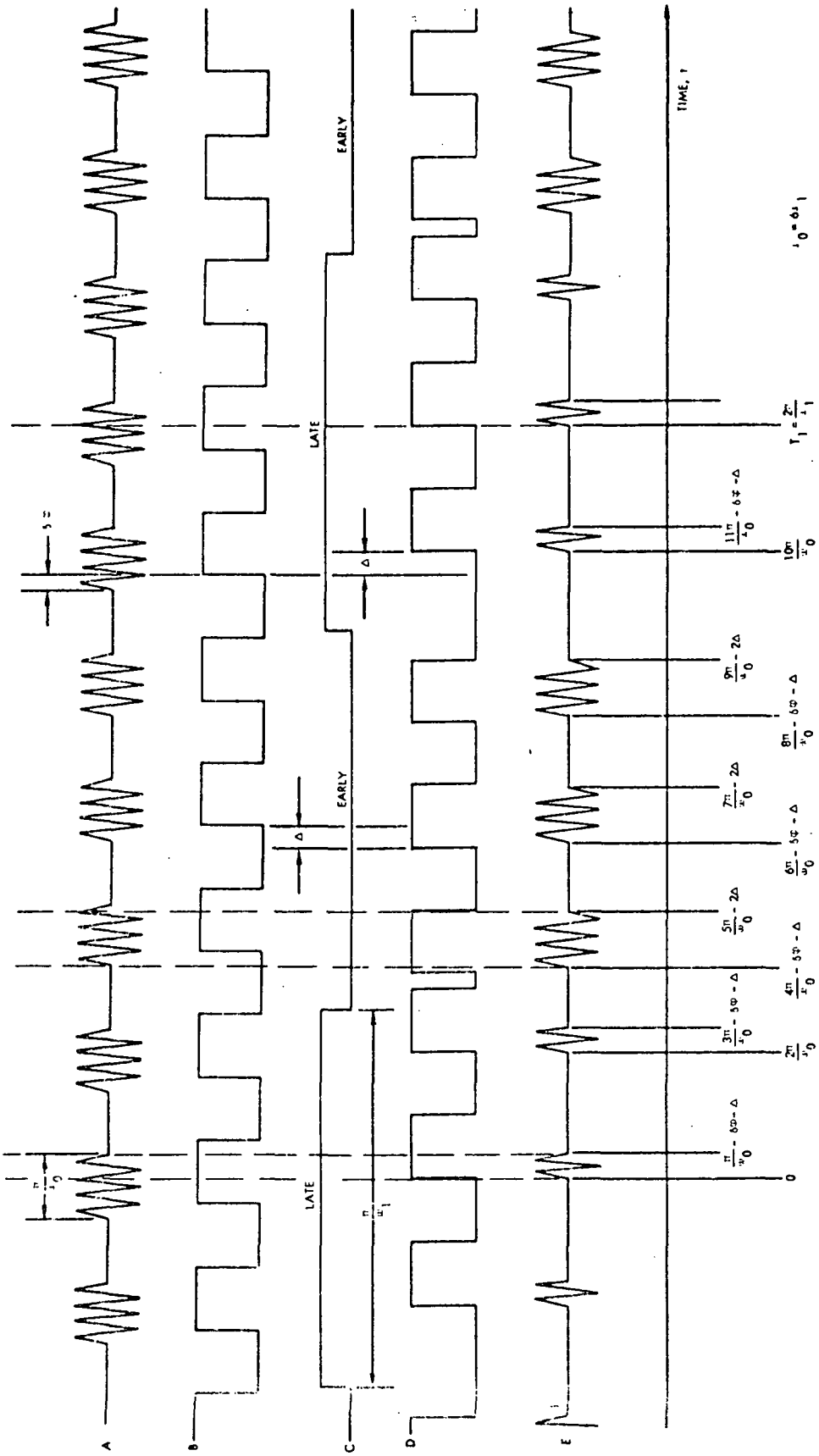

Figure A.2-8. Circuit Waveforms for "Fine-Tone" Tracker Mode

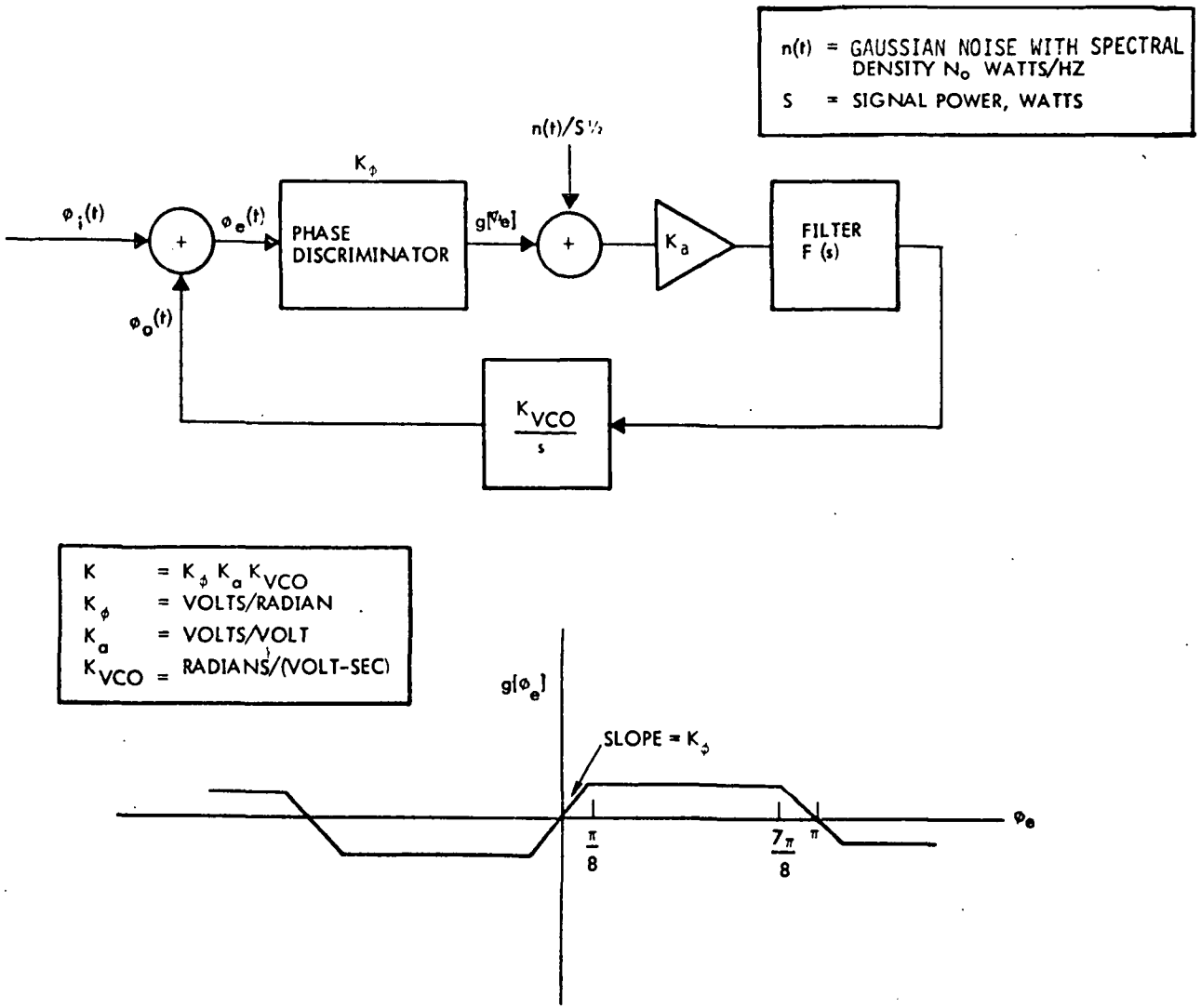

Figure A.2-9. Early-Late Gate Tracking Model

where

$\overline{\theta}_{no}$ = rms phase errors

S = signal power

N = noise power

$\left(\frac{S}{N}\right)_{loop}$ = loop signal to noise ratio.

Eisenhauer and Ridge (Reference A-5) have shown that the signal to noise ratio in the tracking loop is related to the IF signal to noise ratio by the expression below.

$$\left(\frac{S}{N}\right)_{loop} = \frac{\overline{f_{\phi}^2(t)}}{\Phi_{BPF} \cdot B_{loop}} \qquad \text{(A.2-5)}$$

$$= \frac{3.1081 \times 10^{-5} S_{IF}}{0.16217 \left(\frac{B_{loop}}{B_{IF}}\right) N_{IF}}$$

$$= 19.1 \times 10^{-5} \left(\frac{B_{IF}}{B_{loop}}\right)\left(\frac{S_{IF}}{N_{IF}}\right)$$

where

$\overline{f_{\phi}^2(t)}$ = mean squared signal power

B_{IF} = IF noise bandwidth

B_{loop} = loop bandwidth

$\frac{S_{IF}}{N_{IF}} = \left(\frac{S}{N}\right)_{IF}$ = IF signal to noise ratio.

However, in deriving Equation (A.2-5), Eisenhauer and Ridge assumed a perfect envelope detector. In order to achieve the most accurate relationship between loop and IF signal to noise ratios the factor K which relates envelope detector input to envelope detector output must be incorporated in the equation as shown below.

$$\left(\frac{S}{N}\right)_{loop} = 19.1 \times 10^{-5} \quad (K) \left(\frac{B_{IF}}{B_{loop}}\right)\left(\frac{S}{N}\right)_{IF} \qquad \text{(A.2-6)}$$

where the value of K may be found from the curve obtained by Fubini (Reference A-6) and given in Figure A.2-10.

Chang (Reference A-7) derived an expression by which the loop noise bandwidth (B_L) may be evaluated; however the values obtained for loop bandwidth are complicated by the relationship of loop gain, natural frequency, and damping factor. Loop gain is a function of range and is tabulated in Table 1 with other important parameters, i.e., loop bandwidth and natural frequency.

By the use of Equations (A.2-6) and (A.2-4), the phase error as a function of loop signal to noise may be obtained. These equations are valid for loop signal to noise ratios greater than 6 dB. Below loop signal to noise ratios of 6 dB, there is no assurance that the tracking loop is in lock. It has been shown (Reference A-8) that the probability of cycle slip is a minimum of 5% with a loop signal to noise ratio of 5 dB. With uncertainty probabilities of this magnitude (5%), range information can not be considered valid. Therefore, a model for use in predicting the range tracking performance when loop signal to noise ratios are below 6 dB would not be particularly useful.

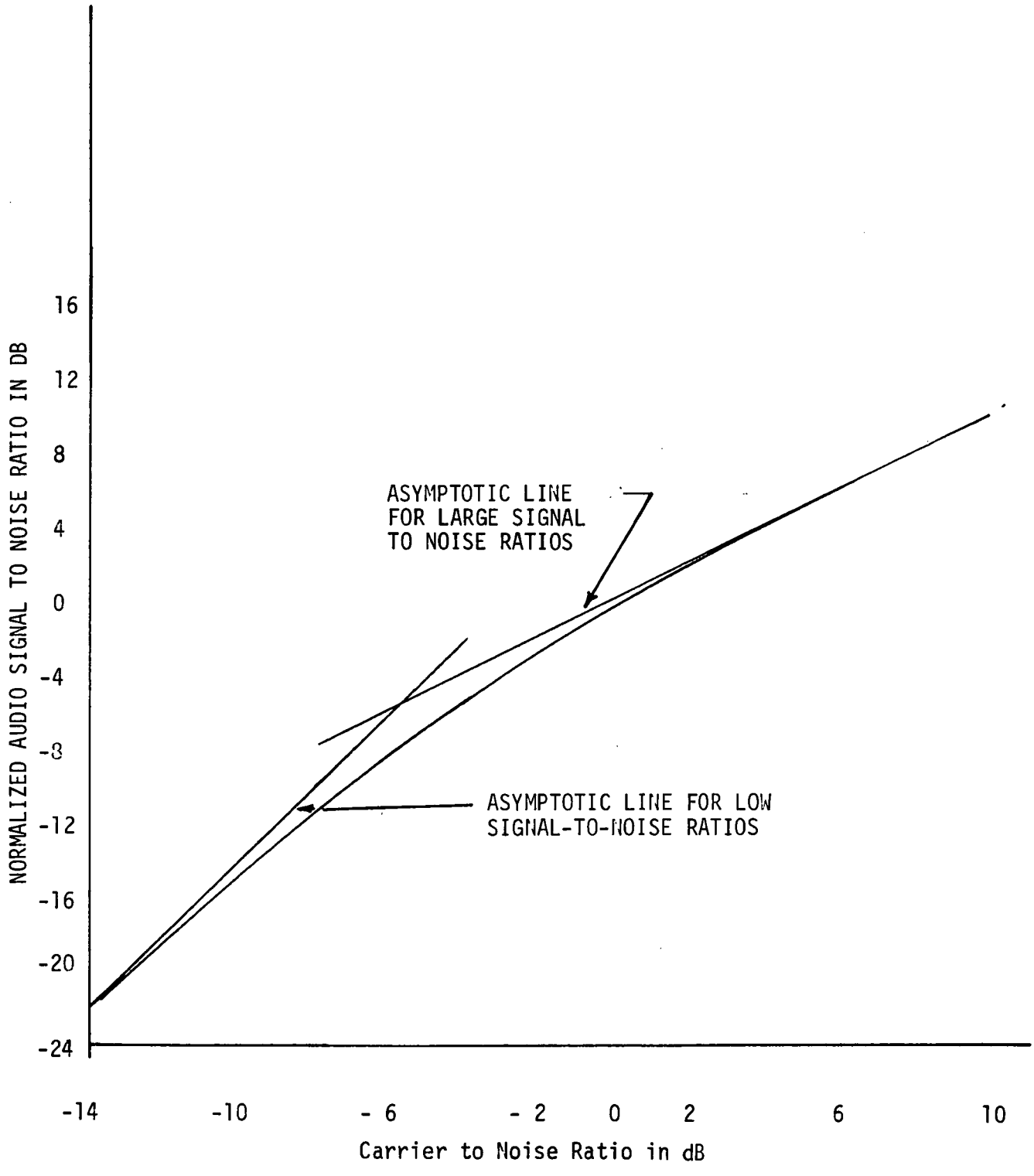

Figure A.2-10. Envelope Detector Degradation Factor (Reference A-6)

A.3 SUMMARY

A mathematical model of the VHF Early/Late gate tracking loop has been presented which is valid for signal to noise ratios greater than 6 dB. Since the phase lock loop which is the basis for the model does not have a high probability of track at signal to noise ratios below 6 dB, a math model for use when signal to noise ratios are low would not be particularly useful.

REFERENCES

A-1. U. S. Government Memorandum, "Fourth Status Report on VHF Ranging," December 1967.

A-2. TRW IOC 7323.2-207, "Analysis of the Fine Tone Tracker," Y. Z. Viscanta, December 5, 1967.

A-3. TRW IOC 7131.57-2, "Probability of Acquisition in the LM Fine Tracking Loop," J. L. Lewis, 19 December 1972.

A-4. Gardner, Floyd M., Theory of Phase Lock Techniques as Applied to Aerospace Transponders, Contract No. NAS 8-11509, George C. Marshall, Space Flight Center, NASA.

A-5. TRW IOC No. 72:7153.6-88, "Signal-to-Noise Ratio Analysis of the Fine Tone Tracking Loop of the VHF Ranging System," D. R. Eisenhauer and L. K. Ridge.

A-6. Fubini, Eugene G., "Signal to Noise Ratio in AM Receivers," Proceedings of the IRE, December 1948.

A-7. TRW IOC No. 68-7251-CC-125, "VHF Ranging Error Analysis," C. Y. Chang, 1 November 1967.

A-8. TRW Report No. 11176-H042-R0-00, Bi-Monthly Technical Report No. 2, Volume II, 1 October 1969.

APPENDIX B

VHF RANGING SYSTEM-UNLOCK PROBABILITY

APPENDIX B

VHF RANGING SYSTEM-UNLOCK PROBABILITY

B.1 INTRODUCTION

This appendix summarizes the conclusions of Sannemon and Rowbotham (Reference B-1) regarding the unlock probability of a phase locked loop operating near threshold, lists many of the parameters to be used in the analysis and presents the equations required in modelling the phase locked loop.

B.2 UNLOCK PROBABILITY MATHEMATICAL MODEL

The output phase jitter of a phase locked loop increases as the loop signal to noise ratio decreases. Since the phase detector of the phase locked loop has only a limited range of operation the loop will drop out of lock when phase error exceeds the operational range of the loop. The range error which may be expected as a result of phase jitter has been examined in Task 3 (Range Error Sources). This section of this Appendix presents a discussion of the probability of unlock [P(unlock)] of the phase locked loop.

A study by Sannemon and Rowbotham (Reference B-1) has resulted in the development of some empirical relationships which are used herein as a basis for the Unlock Probability Mathematical Models.

Sannemon and Rowbotham (Reference B-1) obtained an empirical formula for mean time to unlock near thresholds of a high gain, second order phase lock loop, with a damping factor of .707 and zero initial error as given below:

$$T_{av} = \frac{2}{\omega_n} \exp \left[\pi \ (SNR)_L \right] , \qquad \text{(B.2-1)}$$

where ω_n = natural radian frequency of the loop

$(SNR)_L$ = loop signal to noise ratio, and

T_{av} = average elapsed time to skip one cycle

Also, in their study Sannemon and Rowbotham have found that an exponential of the form

$$P(\text{unlock}) = 1 - \exp \left[\frac{-T}{T_{av}} \right] \qquad \text{(B.2-2)}$$

is a good representation of the probability that the phase locked loop has skipped a cycle (unlocked). The quantity P(unlock) is the probability that the loop has skipped a cycle after time T has elapsed.

Equations B.2-1 and B.2-2 will be used as math models in the analysis of Unlock Probability. Parameters given in the following sections of this appendix will be utilized in computing Unlock Probability.

B.3 VHF RANGING SYSTEM PARAMETERS

Parameters descriptive of the ASTP Ranging System (particularly RF characteristics) have been extracted from Reference B-4 and are presented in Table B-1. These parameters do not differ greatly from the parameters of the Apollo VHF ranging system and will be the basis of calculations performed in the analytical model.

Parameters	Apollo to Soyuz spacecraft		Soyuz to Apollo spacecraft	
	Apollo transmit	Soyuz receive	Soyuz transmit	Apollo receive
Antenna gain	$\geq$ -3 dB over 80 percent of sphere with well-timed manual switching between antennas and $\geq$ -1 dB for look angles of θ = 35° ± 10° and θ = 180° ±10°	$\geq$ -5 dB over 80 percent of sphere with well-timed manual switching of antennas and $\geq$ -3 dB for look angles of θ = 10° ± 5° and ϕ = 180° ± 5°	$\geq$ -5 dB over 80 percent of sphere with well-timed manual switching of antennas and $\geq$ -3 dB for look angles of θ = 10° ± 5° and ϕ = 180° ± 5°	$\geq$ -3 dB over 80 percent of sphere with well-timed manual switching between antennas and $\geq$ -1 dB for look angles of θ = 35° ± 10° and ϕ = 180° ± 10°
Antenna polarization	Linear	Right circular	Right circular	Linear
Carrier frequency	259.7 MHz	259.7 MHz	296.8 MHz	296.8 MHz
Maximum frequency instability of the transmitters and receiver hetrodynes	+0.003%	±0.003 %	±0.003%	±0.003%
System noise temperature	NA	1200° K	NA	1200° K
Circuit loss (from transmitter or receiver to antenna)	4.5 dB	3.8 dB	3.8 dB	4.5 dB
Receiver noise bandwidth (IF)	NA	70 kHz	NA	70 kHz
Transmitter output power	10 W, peak (minimum)		10 W, peak (minimum)	
Minimum required power at the receiver input		-104.5 dBm		-105.7 dBm
Receiver noise figure		6 dB		6 dB

Table B-1. VHF Ranging System Parameters

Parameters	Apollo to Soyuz spacecraft		Soyuz to Apollo spacecraft	
	Apollo transmit	Soyuz receive	Soyuz transmit	Apollo receive
Modulation type	AM (carrier keyed on/off)		AM (carrier keyed on/off)	
Percent modulation of carrier	100%	NA	100%	NA
Ranging tones				
Coarse	3.95 kHz/247 Hz modulo - two-sum squarewave		3.95 kHz/247 Hz modulo - two-sum squarewave	
Medium	3.95 kHz squarewave		3.95 kHz squarewave	
Fine	31.6 kHz squareware		31.6 kHz squarewave	
Ranging time delay variation (31.6 kHz fine tone)			No more than 300×10^{-9} seconds	

Table B-1. VHF Ranging System Parameters (continued)

REFERENCES

B-1. Sannemon, R. W. and J. R. Rowbotham, "Unlock Characteristics of the Optimum Type II Phase Locked Loop," Transactions IEEE, Volume ANE-11, pp. 15-24, March 1964.

B-2. "Apollo VHF Critical Design Review," RCA Defense Communications Systems Division, RMM-CDR-1, 28 February 1968.

B-3. Chang, C. Y., "VHF Ranging Error Analysis," TRW IOC 68-7251-CC-125, 1 November 1968.

B-4. Apollo/Soyuz Test Project, "Interface Signal Characteristics for the Radio Communications and Ranging System," IED 50102, 2 December 1972.

B-5. TRW IOC 73:7153.6-77, "ASTP VHF Ranging System - Early/Late Gate Math Model," 25 May 1963.

B-6. TRW IOC 73:7153.6-96, "Error Sources in VHF Ranging," 28 June 1973.

APPENDIX C

SYSTEM ERROR MODEL DEVELOPMENT AND EVALUATION

APPENDIX C

SYSTEM ERROR MODEL DEVELOPMENT AND EVALUATION

C.1 INTRODUCTION

The range error analysis presented in this appendix when integrated with the Early/Late Gate Mathematical Model will permit the performance of the VHF ranging system to be predicted.

C.2 ERROR SOURCES AND MEASUREMENT PARAMETERS

A systematic procedure is required for evaluating the effects of the various factors contributing to errors in range measurement in order to accurately and reliably predict ranging system performance under a wide variety of input carrier levels and signal to noise ratios.

There are six primary sources of ranging error which will be considered in the development of the system model. These primary error sources are:

1) System signal to noise ratio
2) Vehicle motion
3) Oscillator instability
4) Granularity or resolution
5) Variations in phase delays, and
6) Error due to the simultaneous transmission of Voice and Ranging Information.

Each of these error sources will be discussed in the following sections.

C.2.1 Range Error Due to System Signal to Noise Ratio

The range error caused by random noise results from phase jitter introduced in the range tone tracking loops in both vehicles. Since the Soyuz spacecraft contains the ranging transponder, the jitter in the transponder tracking loop is transmitted to the CSM. Therefore, range error is a complex function related to the transfer characteristics of CSM and Soyuz circuitry, the receiver bandwidth, etc. Chang (Reference C-1) has derived a relationship between range error and loop characteristic as follows:

$$\sigma_{RSNR} = \frac{c}{2\omega\sqrt{2(S/N)_{LOOP}}} \left[1 + \frac{T_S B_{SC}}{T_C B_C}\right]^{1/2} \qquad (C.2\text{-}1)$$

where

σ_{RSNR} = range error in meters, due to loop signal to noise

c = velocity of light in meters/sec.

ω = tracking tone frequency

$(S/N)_{LOOP}$ = CSM loop signal to noise ratio

T_S, T_C = system noise temperature in Soyuz and CSM spacecraft, respectively

B_C = CSM tracking loop one sided equivalent bandwidth, and

B_{SC} = cascaded one sided equivalent noise bandwidth of the tracking loops in the two vehicles.

Equation C.2-1 is a useful mathematical model, valid when the loop signal to noise ratio is greater than 6.0 dB. However, it has been shown in References C.2 and C.3 that the accuracy of a phase locked loop range tracker is poor when the loop signal to noise ratio is less than 6 dB due to the increasingly high probability of cycle clip as loop signal to noise ratio decreases. Due to the fact that the phased locked loop may not be "locked on" the carrier frequency when the loop signal to noise ratio is less than 6 dB, a mathematical model of the phase locked loop for loop signal to noise ratios less than 6 dB would not be particularly useful.

C.2.2 Range Error Due to Relative Spacecraft Motion

The steady state range error is the result of the relative motion between space vehicles and is affected by spacecraft velocity and acceleration. These error sources are discussed in the following subsections.

C.2.2.1 Range Error Due to Relative Velocity between Spacecraft

The steady state range error due to a constant relative velocity between the two spacecraft may be determined by examining the relationship between actual range, measured range, and the tracking loop transfer functions.

Consider the system having an input r(t), a transfer function h(t), and an output $r_m(t)$ as shown below:

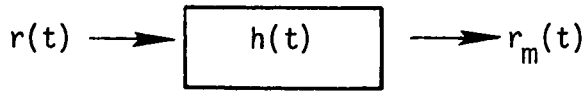

The relationship between input and output of the tracking loop may be stated mathematically as

$$r_m(t) = r(t) * h(t) \qquad \text{(C.2-2)}$$

where

$r_m(t)$ = measured range

r(t) = actual range

* = convolution, and

h(t) = tracking loop transfer function.

The Laplace transform of $r_m(t)$ is

$$L[r_m(t)] = R(s) \cdot G_C(s) \qquad \text{(C.2-3)}$$

where

$R_{(s)}$ = Laplace transform of r(t), and

$G_C(s)$ = Laplace transform of h(t)

$$= \frac{\frac{s}{2.27} + 1}{\frac{s^2}{0.1853K} + \left[\frac{1}{K} + \frac{1}{2.27}\right] s + 1} \qquad \text{(C.2-4)}$$

(Reference C-1)

where K = tracking loop gain.

The actual range between the spacecraft may be specified in a general form in terms of system parameters as in Equation C.2-5.

$$r(t) = R_o + vt + \frac{1}{2} at^2 \qquad \text{(C.2-5)}$$

where

r_o = initial range

v = relative spacecraft velocity, and

a = relative spacecraft acceleration.

To determine the steady state range error due to a constant relative velocity between the spacecraft, acceleration may be assumed zero, allowing Equation C.2-5 to be reduced to

$$r(t) = R_o + vt \ . \qquad \text{(C.2-6)}$$

The Laplace transform of r(t) then is

$$L[r(t)] = R(s)$$

$$R(s) = \frac{R_o}{s} + \frac{V}{s^2} \ . \qquad \text{(C.2-7)}$$

Substituting Equation (C.2-7) into (C.2-3) gives

$$L[r_m(t)] = \left(\frac{R_o}{s} + \frac{V}{s^2}\right)\left(\frac{\frac{s}{2.27} + 1}{\frac{s^2}{0.1853K} + \left[\frac{1}{K} + \frac{1}{2.27}\right] s+1}\right) \qquad \text{(C.2-8)}$$

Applying the Laplace final value theorem to Equation (C.2-8) as shown in Reference C-1 allows the steady state velocity error (σ_{RV}) to be determined; that is,

$$\sigma_{RV} = \frac{V}{K} \text{ ft} \ . \qquad \text{(C.2-9)}$$

C.2.2.2 Range Error Due to Acceleration between Spacecraft

The range error (σ_{RA}) due to the relative acceleration between spacecraft may be obtained by multiplying the Laplace transforms of the tracking loop transfer function h(t) and the input function r(t); and, then applying the Laplace final value theorem as follows:

$$\sigma_{RA}(s) = \left(\frac{R_o}{s} + \frac{V_o}{s^2} + \frac{3A}{s^3}\right) \frac{\frac{s^2}{0.1835K} + \frac{s}{K}}{\frac{s^2}{0.1835K} + \left[\frac{1}{K} + \frac{1}{2.27}\right] s+1} \qquad \text{(C.2-10)}$$

where V_o is the initial velocity of the spacecraft and A is assumed to be a constant acceleration. Applying the Laplace final value theorem gives

$$\sigma_{RA}(s) = \lim_{s \to 0} L[sf(s)] \qquad \text{(C.2-11)}$$

$$= \frac{V_o}{K} + \frac{3A}{0.1835K} + \cancel{\frac{3A}{sK}} \text{ undefined as } s \to 0$$

Equation C.2-11 shows that as two spacecraft close or separate in range at a constant acceleration, the range error in the tracking loop becomes infinitely large. That is, the VHF tracking loop cannot track a constant acceleration for an unlimited time.

C.2.3 Range Errors Due to Oscillator Instability

The range between two spacecraft is a function of the phase shift between the transmitted and received ranging tone and can be calculated (Reference C-4) by the use of Equation (C.2-12) below:

$$R = \frac{c}{4\pi f} [\phi + 2n\pi] \ , \qquad \text{(C.2-12)}$$

where

c = velocity of light

f = ranging tone frequency

ϕ = measured phase shift between transmitted and received ranging tones at the CSM, and

n = integer number of cycles of delay in round trip from CSM to transponder and back.

In order to obtain the range deviation as a function of frequency change, we may take the derivative of R with respect to f which gives

$$\frac{dR}{df} = R\left(-\frac{1}{f}\right) , \qquad \text{(C.2-13)}$$

which may be rewritten

$$dR = R\left(-\frac{df}{f}\right) . \qquad \text{(C.2-14)}$$

Equation (C.2-14) agrees with the estimate of master clock oscillator stability by Gerber (Reference C-5). Given a ranging tone oscillator stability of $\frac{df}{f} = 10^{-6}$, the corresponding range error is

$$\sigma_{RO} = 10^{-6}R. \qquad \text{(C.2-15)}$$

However, in addition to a range error due to master clock instability, a range error may result from a frequency bias error introduced in the phase lock loop by a noisy incoming signal. Ranging error due to frequency offset would appear to the CSM phase measuring equipment as a steady state velocity shift. But an error resulting from frequency offset can not be distinguished from the error due to relative spacecraft motion and may be computed by equation (C.2-9).

C.3 RANGE ERROR SUMMATION

The principal sources of range measurement errors in the VHF ranging system have been identified as

1) System signal to noise ratio

2) Vehicle motion

3) Oscillator instability

4) Granularity

5) Phase delays, and

6) Simultaneous transmission of voice and ranging information.

The total range error as a result of each of the six identifiable contributions may be determined by obtaining the square root of the sum of the squares if, and only if, the error contributions are independent.

It may be shown by means of partial derivatives that range errors due to relative velocity between spacecraft, oscillator stability, granularity, and circuit delays are functionally independent of each other. However, range errors due to signal to noise ratio, frequency offset, and signal intermodulation may not be functionally independent. Therefore, in order to determine the total rms range error in the VHF range system, errors due to signal to noise ratio, frequency offset, and signal intermodulation should be computed as a function of range. Due to the difficulty in calculating the correlation coefficients between the error sources, statistical and functional independent of error sources will be assumed, so that the rms range error can be determined by obtaining the square root of the sum of the squares (rss) of the errors. The rss errors obtained as described should be compared to actual range errors determined from available data. If correlation between calculated error values and real data are within a specified tolerance, it can be assumed that the rss method of determining error is suitable for use in this ranging system analysis.

C.2.4 Ranging Error Due to Granularity (Phase Resolution)

The phase shifting system in the CSM fine tone tracking loop employs a digital countdown from 2.02 MHz and a four-tap delay line for deriving the final phase reference used in comparing the phase of the received and transmitted ranging tones. The smallest increment to which range can be resolved is thus determined by one-fourth of a 2.02 MHz cycle, or 60.8 ft. The maximum range error due to this readout granularity (σ_{RG}) is plus or minus one-half increment, or $\pm$ 30.4 ft. If this range error is considered to be a random variable uniformly distributed in probability over the interval $\pm$ 30.4 ft., the resultant rms error is $60.8/\sqrt{12}$, or 17.6 ft.

Granularity error is not a function of range and exists only at the CSM where the range measurement is performed. No source of granularity error other than the primary clock has been found; therefore, the rms granularity error used throughout these analyses is as given in the preceding; i.e., 17.6 feet.

C.2.5 Ranging Error Due to Phase Delay Variations

Signal delays are introduced by various elements within the ranging system, such as in the transmitters, receivers, antenna cables, diplexer, triplexer, and RF/IF circuits. These delays vary from one set of hardware to the next, vary with temperature and other environmental conditions, and in some cases vary with the received signal level. The effect of most of this delay, the "constant" bias, can be removed by subtracting from the final range readout the results of a zero calibration measurement. The remaining "variable" delay will contribute to measured range errors.

If the total rms time delay variation is 100 nsec, the corresponding rms range error is

$$\sigma_{bias} = 49.3 \text{ ft.} \qquad \text{(C.2-16)}$$

Test data have not been obtained which would allow limiting values or tolerances on bias error to be established. However, such data may well be obtained and incorporated in the report before the final project report is due.

C.2.6 Range Error Due to the Simultaneous Transmission of Voice and Ranging Information

A detailed analysis of the operation of the VHF ranging system when ranging and voice information simultaneously modulate the VHF carrier has been presented in Reference C-2. The results obtained in the analysis indicate that the third order intermodulation product is the primary cause of range accuracy degradation. Equation (C.2-17) gives the rms range error which results from the intermodulation product of voice and ranging signals:

$$\sigma_{TI} = \frac{c}{2\omega_r\sqrt{2(SNR)_L}} \quad , \tag{C.2-17}$$

where

c = 10^9 ft/s,

ω_r = radian frequency of the 31.6 kHz ranging tone, and

$(SNR)_L$ = tracking loop signal to noise ratio.

A range error of 34.4 feet was obtained using equation (C.2-17) in an analysis (Reference C-2), wherein the third order intermodulation product was shown to have a signal to noise ratio of 34.2 dB in the tracking loop bandwidth.

C.4 SUMMARY AND CONCLUSIONS

The primary sources of range measurement error in the VHF Ranging System have been identified and have been assumed to be statistically and functionally independent.

REFERENCES

C-1. TRW IOC No. 68:1251:CC:125, "VHF Ranging Error Analysis," C. Y. Chang, 1 November 1967.

C-2. TRW Report No. 11176-H042-R0-00, Bimonthly Technical Report, Number 2, Volume 11, 1 October 1968.

C-3. TRW IOC No. 73:7153.6-77, "ASTP VHF Ranging System - Early/Late Gate Math Model," M. R. Ellis, 25 May 1973.

C-4. TRW Technical Proposal 24339.00, ASTP Ranging System Mathematical Model Development, January 1973.

C-5. Gerber, E. A. and R. A. Sykes, "State of the Art - Quartz Crystal Units and Oscillators," Proceedings of the IEEE, Vol. 54, No. 2, February 1966, pp. 103-116.

C-6. TRW Report No. 11176-H168-R0-00, Bimonthly Technical Report, Number 4, Volume 1, 5 March 1969.

APPENDIX D

PROBABILITY OF ACQUISITION AND ACQUISITION TIME MATH MODEL

APPENDIX D

PROBABILITY OF ACQUISITION AND ACQUISITION TIME MATH MODEL

D.1 INTRODUCTION

In order to accurately evaluate the performance of the VHF Ranging System, the system acquisition time must be determined as a function of received signal to noise ratio.

This appendix presents a discussion of VHF ranging acquisition, a discussion of the acquisition problem, and a discussion of acquisition time as a function of signal to noise ratio.

D.2 DESCRIPTION OF THE VHF RANGING OPERATION

The measurement of range between the CSM and Soyuz spacecraft is accomplished by the VHF Ranging System in which three fixed tones modulate the CSM VHF carrier in a preset sequence which assures accurate range information once range track is obtained. The actual measurement of range has been described in Appendix A. The following sections of this appendix describe the acquisition process and limitations of the system.

D.2.1 System Acquisition

The VHF range acquisition program is initiated in the CSM by the transmission of a 3.95 KHz tone which on-off modulates the VHF carrier. If the signal transmitted by the CSM is received in sufficient strength at the Soyuz, a signal sensor configures the Soyuz to demodulate the received signal and to modulate the Soyuz transmitter with the selected intelligence. The Soyuz signal when received by the CSM causes the mid tone tracker to lock up. The CSM then initiates the second step of the acquisition sequence; i.e., the CSM modulates its VHF carrier with the 3.95 KHz mid tone combined modulo-2 with a 247 Hz coarse tone. This composite tone is transponded by the Soyuz (as was the initial 3.95 KHz tone) and is received by the CSM which now "locks up" the 247 Hz tracker as well as the 3.95 KHz tracker.

If the composite ranging signal is being tracked properly by the CSM, the CSM range-tracker ceases to modulate with the 3.95 KHz and 247 Hz tone combination, turns on its 31.6 KHz tone, modulates the CSM/VHF carrier by the 31.6 KHz tone, and gates its receiver at a 31.6 KHz rate. When the 3.95 KHz tone component is no longer received by the Soyuz, the Soyuz tracker attempts to lock with the 31.6 KHz tone signal received from the CSM and gates the Soyuz VHF receiver accordingly. Finally, the Soyuz tracks the 31.6 KHz fine tone and modulates the Soyuz VHF carrier with a "cleaned up" or reconstructed 31.6 KHz signal. The 31.6 KHz signal received by the CSM is detected and counted by the Ranging Counter. The condition has

finally been attained whereby the CSM is tracking a 31.6 KHz signal in which there is a phase shift proportional to the two-way distance between spacecraft. By measurement of the delay between transmitted and received tones, range can be determined as given in Appendix A. Figure D.2-1 is a functional flow diagram of the CSM acquisition sequence logic which has just been described.

The VHF range acquisition sequence is completed in 14 seconds. If acquisition has not occurred, the ranging operation ceases. The CSM pilot may re-initiate the acquisition process by manually depressing the ranging reset button. If acquisition has occurred, range information is displayed on the display unit.

D.2.2 Factors Affecting Acquisition

In order for the VHF ranging system to function; i.e., obtain accurate range information, the acquisition process must be successfully completed and information received at the CSM must be processed properly.

A primary factor in the successful acquisition of the ranging system is the amount of power received by the Soyuz. When the received power at the Soyuz is sufficient to activate the signal sensor (operation described in Section D.2.2), the range tone is transponded by the Soyuz and received by the CSM, allowing the acquisition process to be continued.

Other factors which influence the probability of acquisition and acquisition time are tracking loop signal to noise ratio and frequency (phase) offset between the VCO and incoming reference signal.

D.2.2.1 Signal Sensor

As specified (Reference D-1) an average received ranging signal level of -107 dBm at the Soyuz is required in order to set the signal sensor in the acquisition mode. The probability of acquisition and probability of not acquiring, given a received power at the Soyuz of -107 dBm may be

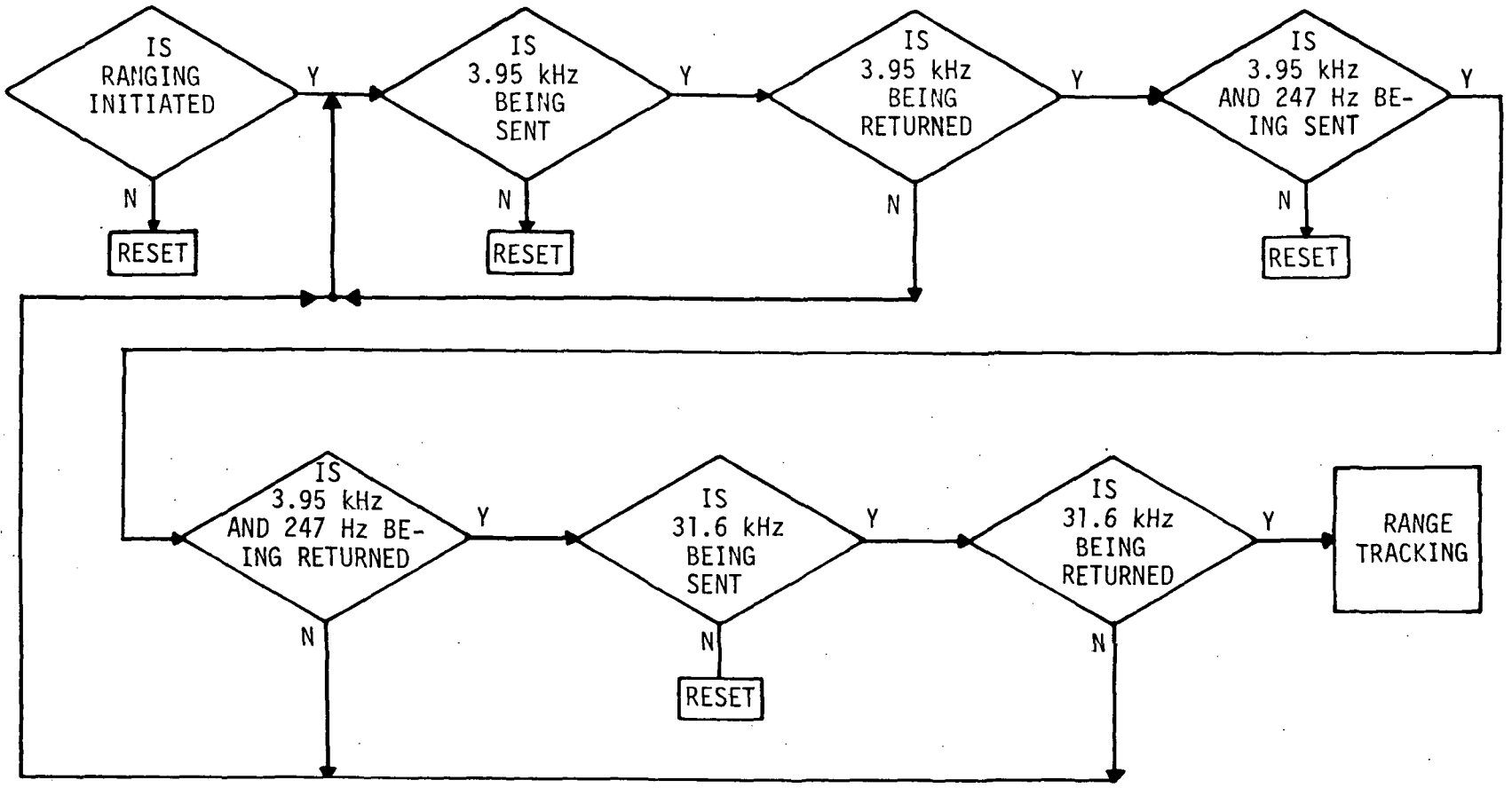

Figure D.2-1 CSM Ranging Acquisition Sequence

stated as follows:

$$\text{If } P_r > -107 \text{ dBm}, \; P_{(ACQ)} \approx 1, \; P_{(\text{NOT ACQ})} \simeq 0, \text{ and}$$

$$\text{If } P_r < -107 \text{ dBm}, \; P_{(ACQ)} = 0, \; P_{(\text{NOT ACQ})} = 1.$$

However, given an average received power at the Soyuz of -107 dBm, the variance in phase lock acquisition time is a function of loop signal to noise ratio and initial frequency (phase) error between the received frequency and the reference frequency.

D.2.2.2 Phase-Lock Loop Acquisition Time

Determining the mean time to acquisition for a second order phase locked loop in a noisy environment is a difficult problem. A careful review of literature describing phase lock loop performance has shown that information describing the distribution of phase lock acquisition time for a small initial frequency error is minimal. The literature study also showed that information describing the second order phase lock loop acquisition time in the presence of narrow band Gaussian noise is minimal.

Formulas have been derived for phase lock acquisition for the noiseless case (References D-2, D-3, and D-4). Based on these formulas certain approximations have been made which have, in the past, been the basis for estimates of mean time to acquisition for the noisy case. However in the VHF ranging model, a curve generated from data obtained from Goldman's (Reference D-5) results is the basis for the determination of acquisition time.

D.2.2.2.1 Analysis of Acquisition Time

The Soyuz fine tone tracking loop has the widest bandwidth of the elements of the VHF Ranging System and is therefore the "weakest link" in the CSM-Soyuz-CSM ranging sequence. The Soyuz transponder actually sets the performance limit of the entire VHF ranging system.

The effect of Soyuz wide bandwidth is to increase the difficulty of lock up (compared to CSM) but at the same time allows acquisition time to be minimal. Therefore, if lock up of the Soyuz tracker can be achieved, there is a high probability that the entire system is capable of lock up. The preceeding may be restated as follows: the conditional probability of acquisition at the CSM assuming acquisition at the Soyuz can be considered near unity. However, because of the statistical nature of noise, there will always be a small probability that a loop will not acquire, even though noise levels may be small.

The system mean time to acquisition may be obtained by summing the individual loop acquisition times of the tracker loops involved. These loops are as follows

1) the CSM mid tone,

2) the CSM mid tone and coarse tone,

3) the Soyuz fine tone, and

4) the CSM fine tone.

The tracker loops in the CSM may be expected to contribute most heavily to system acquisition time, due to their smaller bandwidths and subsequent larger individual loop acquisition times. In the VHF ranging system only 14 seconds are allowed for system acquisition. If lock up of the CSM fine tone has not occurred within this interval, the acquisition sequence is terminated and a new acquisition sequence must be initiated.

D.2.2.2.2 Acquisition in the Noiseless Case

A preliminary analysis (Reference D-6) of phase acquisition in the LM VHF ranging fine tone loop indicated that the range tracking loop could be modelled as a phase-lock loop with a soft limiter phase discriminator characteristic and a second order filter in the feedback path, as shown in Figure D.2.2.

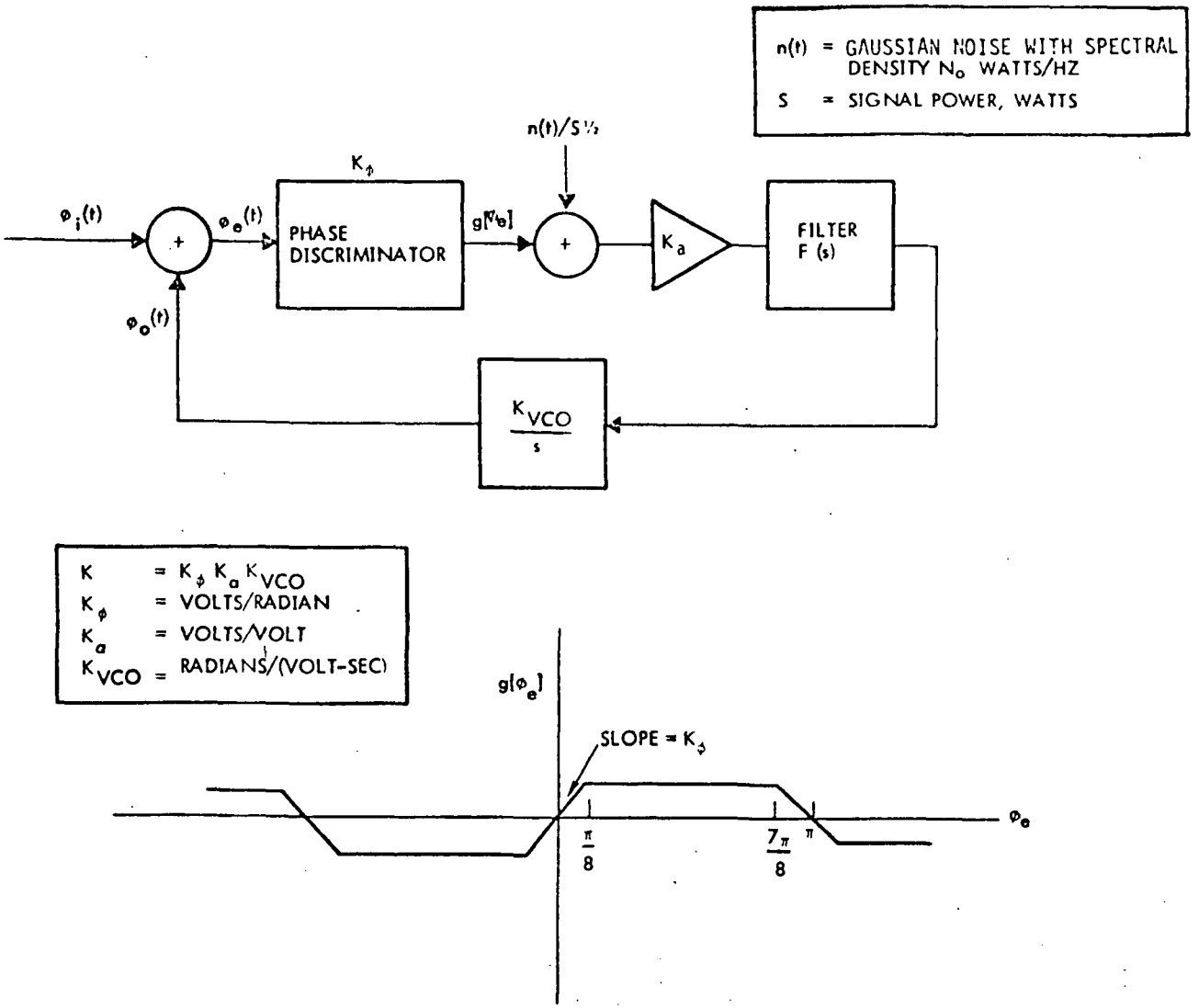

Figure D.2-2. Loop Model and Phase Discriminator

Stiffler (Reference D-7) using a similar model has analyzed the noise free lock up time of a phase lock loop and provides results which give a reasonable estimate of the loop performance in most synchronization applications. A brief summary of the results obtained by Stiffler will follow and the end result; phase lock up time, will be used as a basis for the analysis of lock up of VHF ranging system.

Stiffler by solving the general differential equation

$$\ddot{\phi}(t) + \tau_0 K \cos \phi\ (t)\ \dot{\phi}\ (t) + K \sin \phi\ (t) = 0, \qquad \text{(D.2-1)}$$

of a second order phase lock loop in which τ_0 and K are loop parameters related to loop time constant and loop gain, has derived an expression to determine the phase lock up time for a phase lock loop. He has shown that for a second order loop, phase error $(\theta_e(t))$ is

$$\theta_e\ (t) = 2\ \ \Delta\theta\ \exp \frac{-B_o t}{\sqrt{2}}\ \cos\left(\frac{\sqrt{2}\ B_o t}{2} + \pi/4 \right) \qquad \text{(D.2-2)}$$

where $\Delta\ \theta$ = initial phase error, and

B_o = loop low pass filter band width.

Stiffler shows that the time needed to reduce the error obtained by equation D.2-2 to approximately 1/4 of its original value is

$$T_{\Delta\theta} = \frac{1}{B_L} \qquad \text{(D.2-3)}$$

where B_L is the loop bandwidth of the phase lock loop.

D.2.2.2.3 Acquisition in the Noisy Case

A review of available literature shows several methods which may be applied to the solution for the acquisition time and probability of acquisition for a second order PLL. These methods may be applied to obtain approximate expressions describing phase lock acquisition time in the presence of noise. However, the work by Goldman (Reference D-5) in which the performance of a second order phase lock loop in the presence of narrowband noise was extensively analyzed by means of computer simulations has been chosen as the basis for the acquisition time model for the VHF ranging system.

Goldman utilized an IBM 360 digital computer to solve an expanded form of the integro - differential equation (Eq. D.2-3) which describes a phase-lock loop

$$\dot{\phi}(t) = \theta_i(\tau) - VK_oK_dA \int_o^t \left[\sin\left(\theta_i(\tau) - \theta_o(\tau)\right) + \frac{n_d(\tau)}{A}\right] \cdot f(t-\tau)d\tau \qquad \text{(D.2-3)}$$

where

$\theta_i(\tau)$ = Phase-lock loop (PLL) input phase function.

$\theta_o(\tau)$ = phase jitter

A = rms amplitude of PLL input signal

V = rms amplitude of the voltage controlled oscillator output signal

K_o = VCO gain in radians/volt. second

K_d = phase detector gain in volts/radian, and

$n_d(\tau)$ = PLL input noise voltage.

The expanded equation was solved a total of 4500 times for various loop signal to noise ratios and initial offset errors.

By means of the computer simulations, Goldman was able to obtain plots of percent of acquisition times as a function of acquisition time for various signal to noise ratios and initial phase offset errors. Copies of Goldman's plots are shown in Figures D.2-3a through D.2-7a. These figures show clearly that as loop signal to noise ratio decreases, acquisition time increases and the likelyhood of acquisition decreases. The figures also show the variance in acquisition time which occurred during the simulation for different initial phase offset errors.

Unfortunately, the results obtained by Goldman are not directly applicable to the operation of the ASTP VHF ranging system because Goldman's analysis was performed using an optimum filter characteristic, a constant value of damping factor, and a constant value of phase lock loop gain. Whereas in the ASTP VHF ranging system, it has been shown (Reference D-1) that the parameters of the tracking phase lock loops are not constant, but vary as functions of signal strength.

In order to use the results obtained by Goldman in the VHF math model, the data in the curves (Figures D.2-3a through D.2-7a) is used as a source of data to plot new curves which show the functional relationship between acquisition time (for a 90% probability of acquisition) and loop signal to noise ratio. The curves generated by the use of Goldman's data are shown in Figures D.2-3b through D.2-7b.

Although Goldman's data are replotted in Figures D.2-3b through D.2-7b and the functional relationship between acquisition time and signal to noise ratio is shown, the curves are not in the proper form for use in the VHF model. Because the initial offset between the received ranging frequency and reference frequency in the VHF ranging system is not known and because the time scale for acquisition in the Figures does not truly fit the VHF ranging system, the data presented in Figures D.2-3b through D.2-7b was averaged, plotted as segments of a straight line, and the time scale was revised. Figure D.2-8 is the "averaged" plot from which average acquisition time may be obtained.

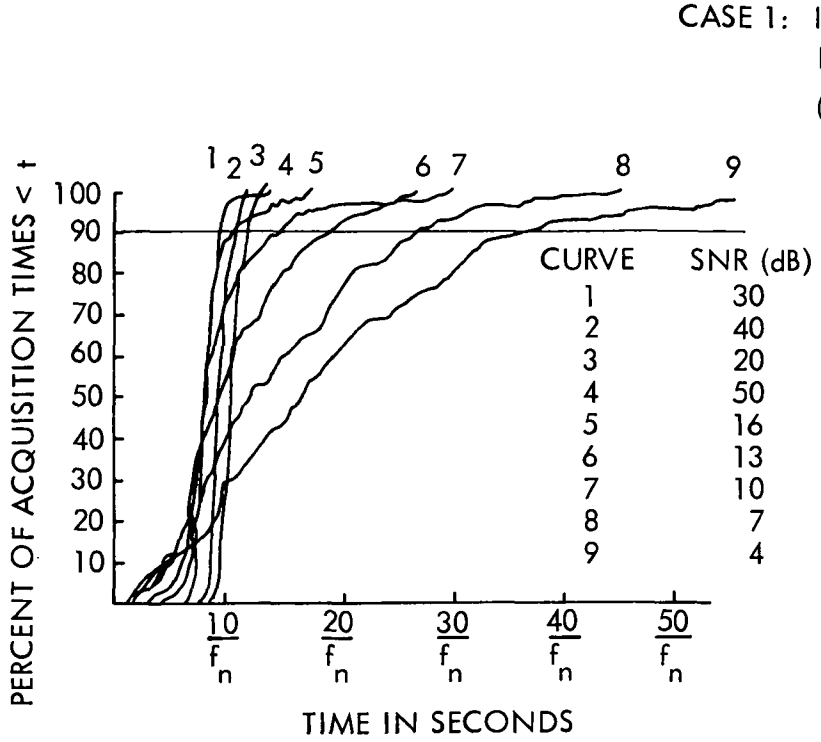

Figure D.2-3a. Per Cent Acquisition Time as a Function of Time for a Second Order Phase Lock Loop (Reference D-5)

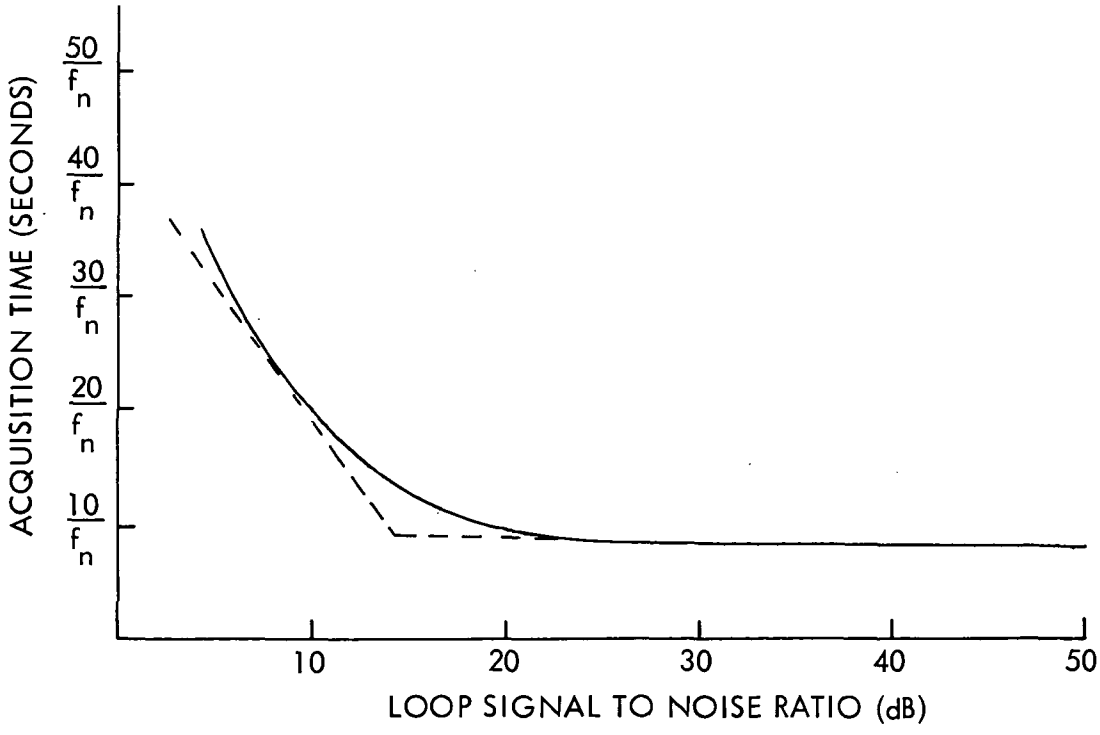

Figure D.2-3b. Acquisition Time (lock probability > 90%) as a Function of Loop Signal to Noise Ratio

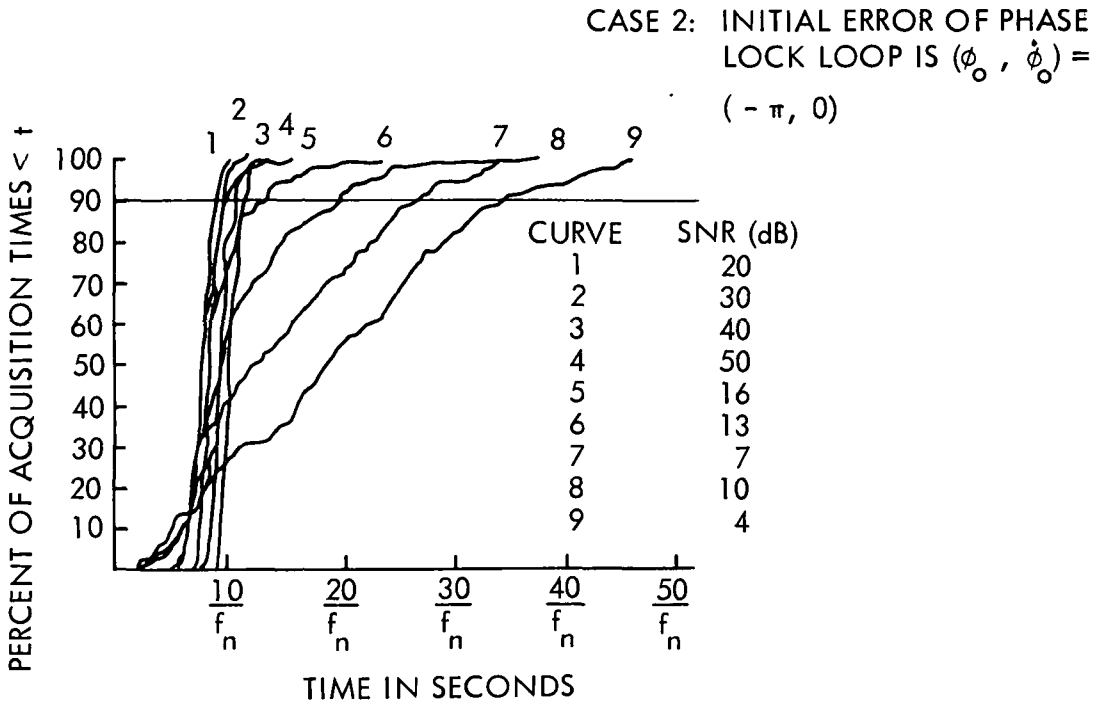

Figure D.2-4a. Percent Acquisition Time as a Function of Time for a Second Order Phase Lock Loop (Reference D-5)

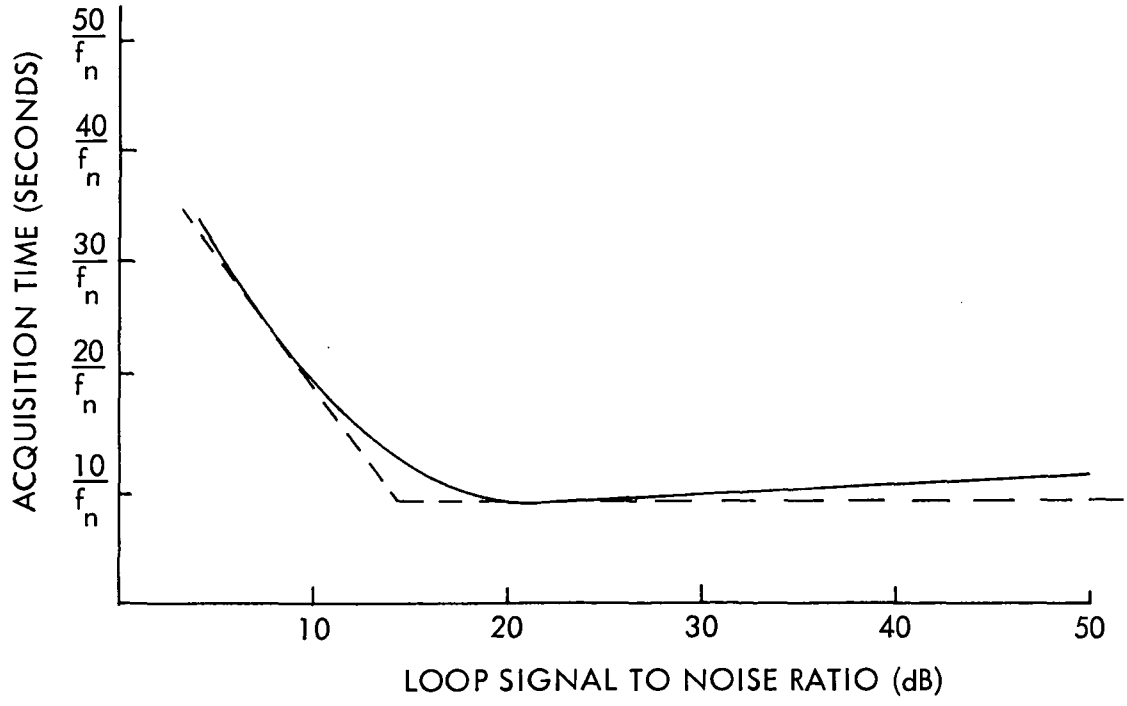

Figure D.2-4b. Acquisition Time (lock probability > 90%) As a Function of Loop Signal to Noise Ratio

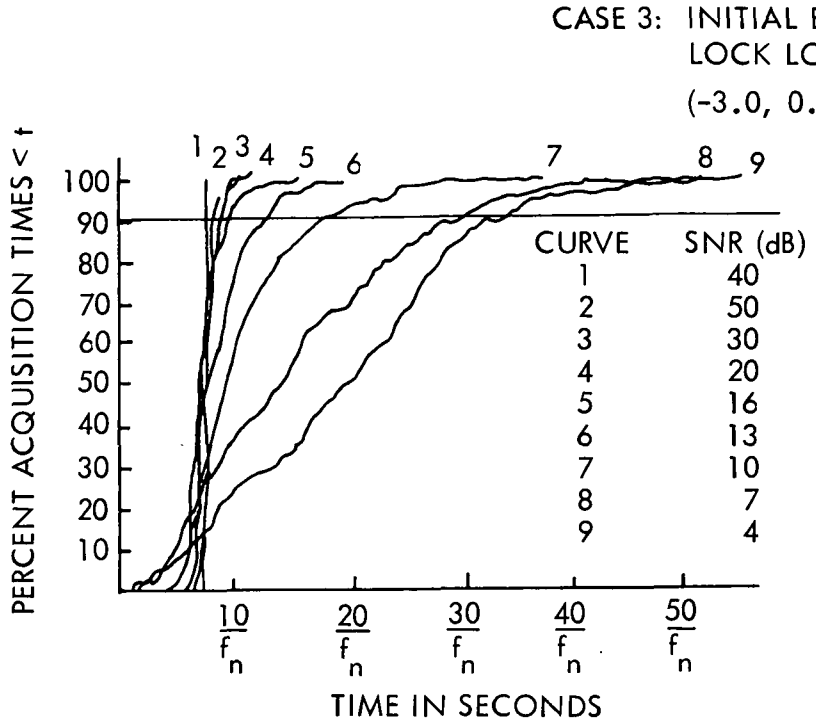

Figure D.2-5a. Percent Acquisition Time <t as a Function of Time for a Second Order Phase Lock Loop (Reference D-5)

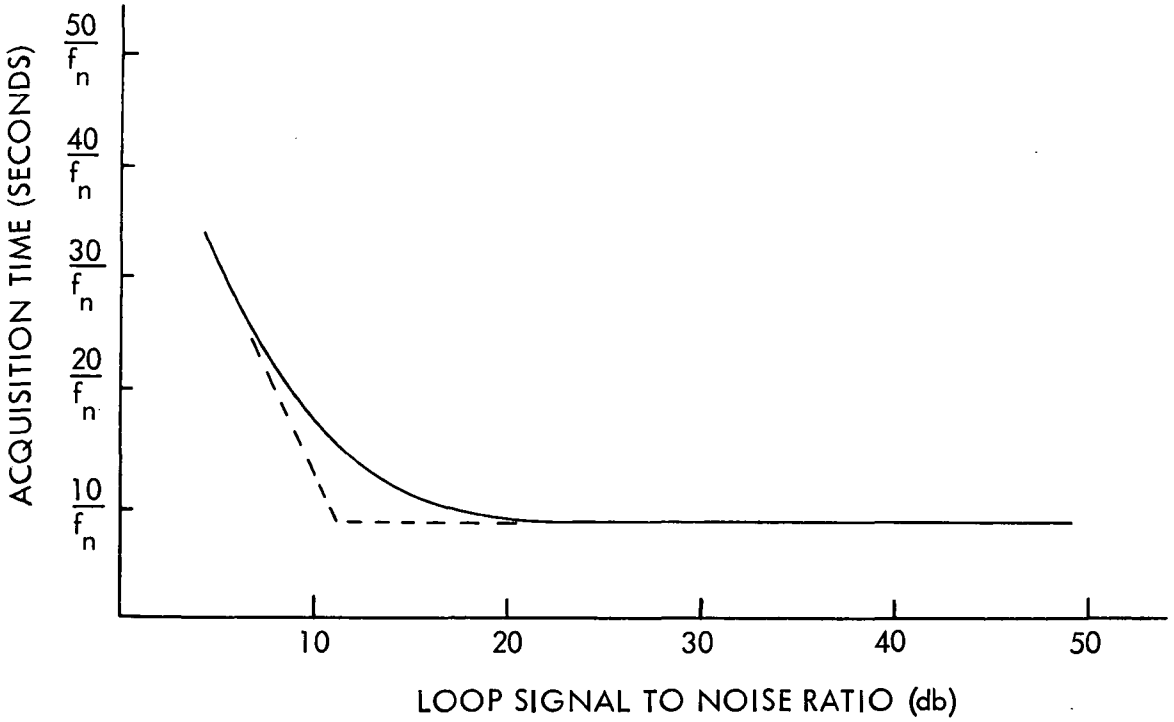

Figure D.2-5b. Acquisition Time (lock probability > 90%) as a Function of Loop Signal to Noise Ratio

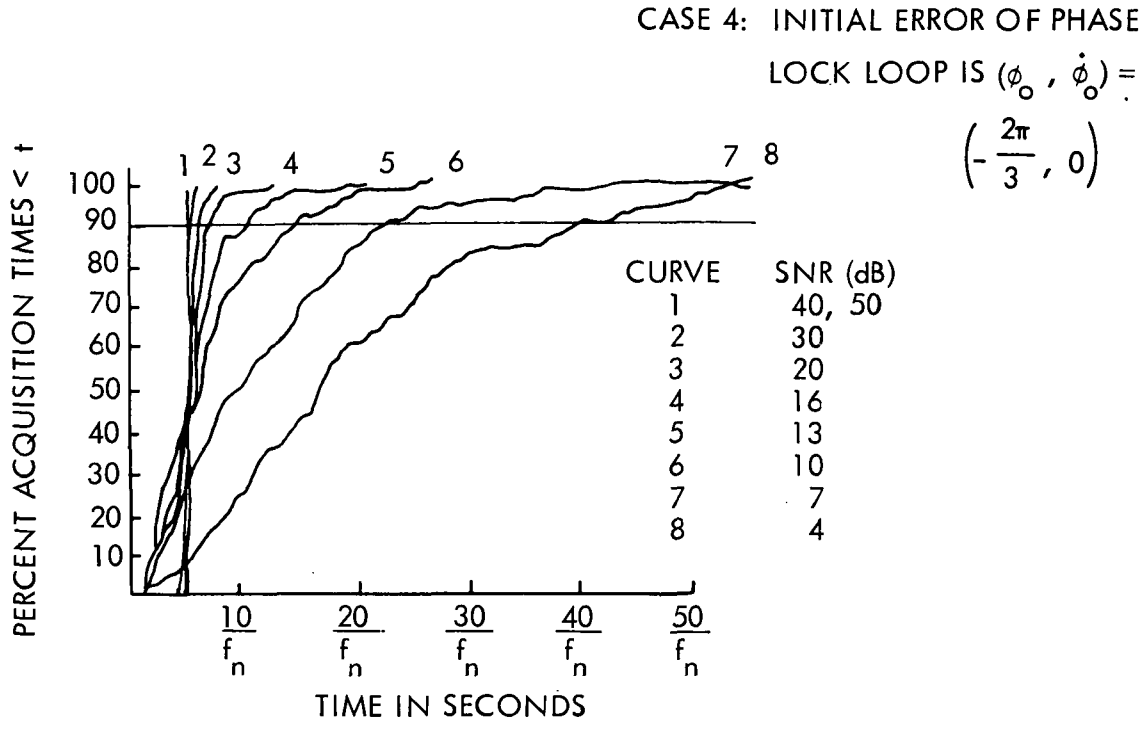

Figure D.2-6a. Percent Acquisition Time < t as a function of Time for a Second Order Phase Lock Loop (Reference D-5)

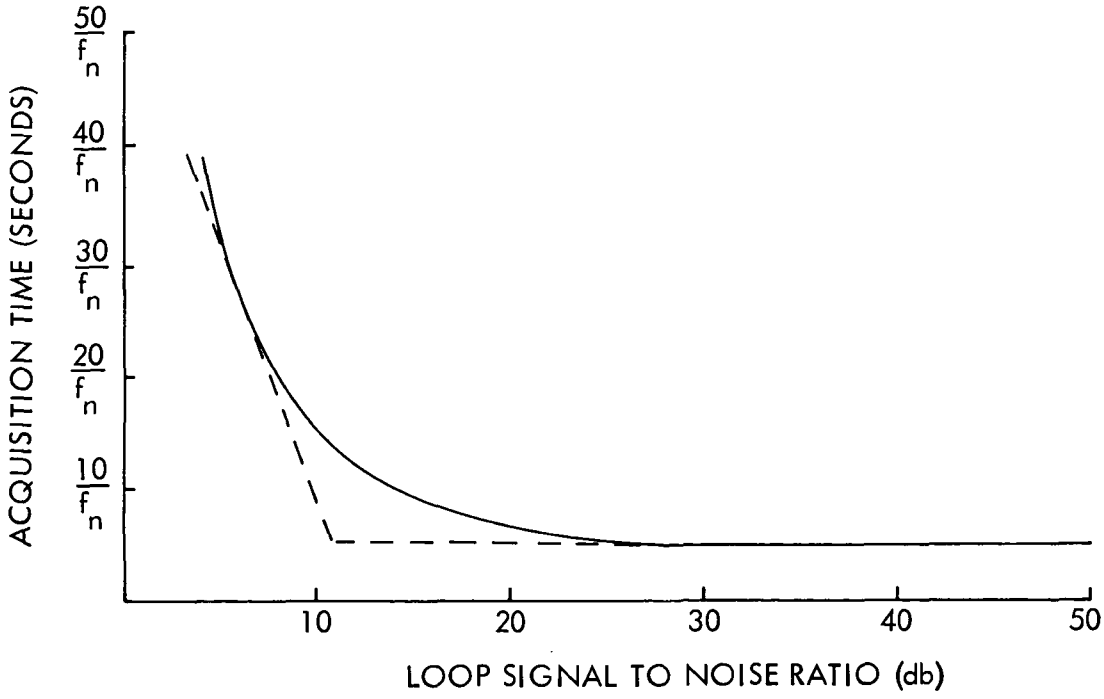

Figure D.2-6b. Acquisition Time (lock probability > 90%) as a Function Loop Signal to Noise Ratio

CASE 5: INITIAL ERROR OF PHASE
LOCK LOOP IS $(\phi_o , \dot{\phi}_o) = (-\frac{\pi}{3} , 0)$

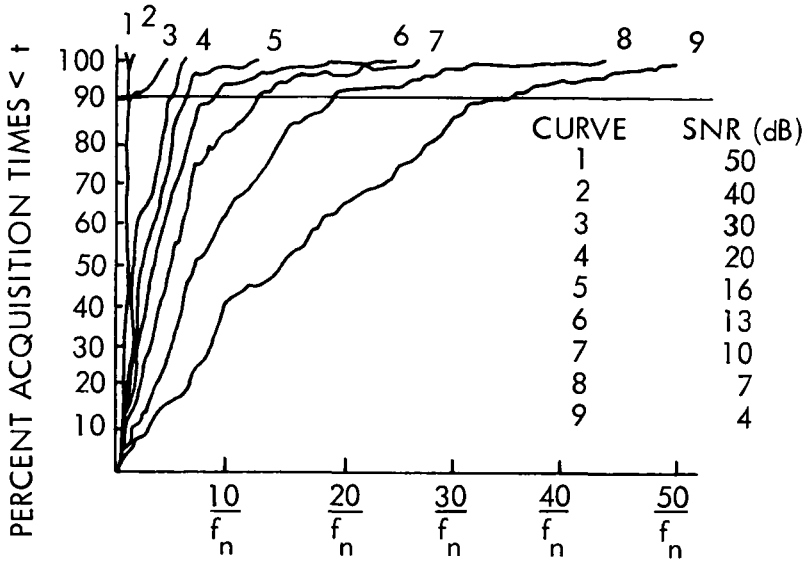

Figure D.2-7a. Percent Acquisition Time < t as a function of Time for a Second Order Phase Lock Loop (Reference D-5)

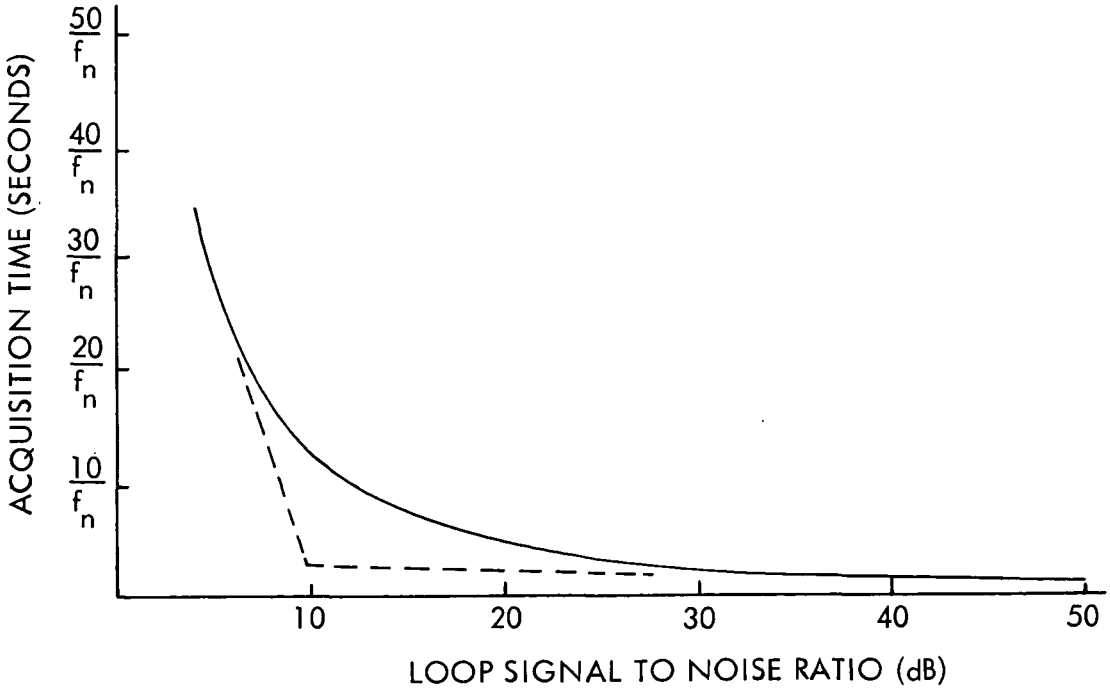

Figure D.2-7b. Acquisition Time (lock probability > 90%) as a Function of Loop Signal-to-Noise Ratio

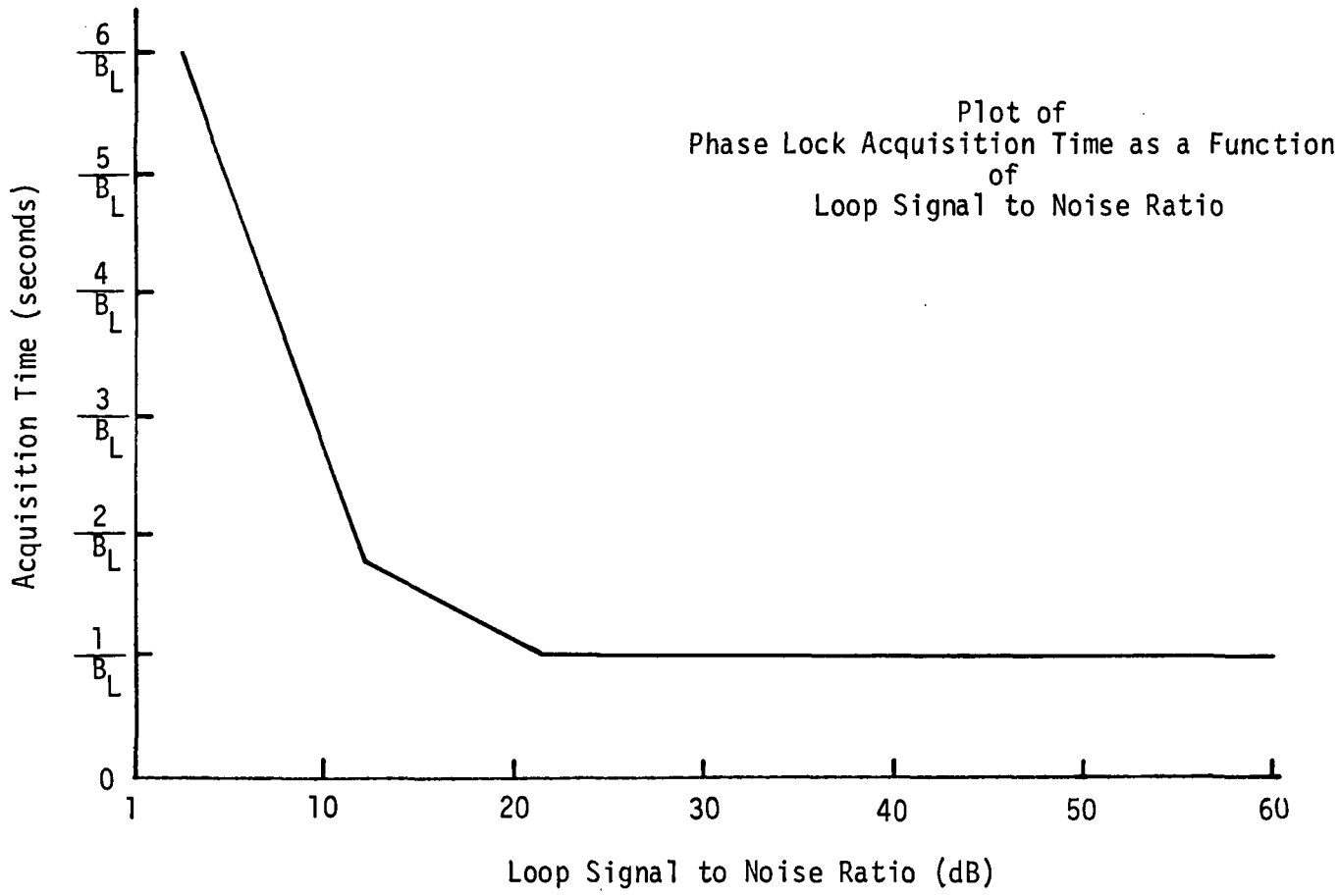

Figure D.2-8 Acquisition Time Model

The time scale utilized in Figure D.2-8 is based on the relationship derived by Stiffler (Reference D-7) and presented in section D.2.2.2.2; i.e., phase lock up time (equation D.2-3) is

$$T_{\Delta\theta} = \frac{1}{B_L} \quad .$$

which gives the acquisition time for a phase-lock loop in a noiseless environment and is used to find the minimum acquisition time which may be obtained by the Functional Model in Figure D.2-7. The single point obtained by Stiffler's equation relates the curve of Figure D.2-8 to a time scale proportional to a VHF ranging system variable parameter, ie. loop bandwidth. Figure D.2-8 is implemented in the mathematical model of the VHF ranging system for the computation of loop acquisition time.

D.3 SUMMARY

The acquisition problem has been examined in detail. At the present time there are no analytical techniques which may be applied to obtain definitive solutions. Therefore, in order to obtain the best possible model for use in the VHF Mathematical Model results obtained by Goldman (Reference D-5) are combined with mathematical derivations by Stiffler and the results incorporated in the model.

REFERENCES

D-1. "Apollo VHF Ranging Critical Design Review," RCA Defense Communications Division, RMM-CDR-1, 28 February 1968.

D-2. Gardner, F. M. and S. S. Kent, "Theory of Phase Lock Techniques as Applied to Aerospace Transponders," NASA Contract NAS-11509.

D-3. Viterbi, A. J., Principle of Coherent Communications, McGraw-Hill, 1966.

D-4. Meer, S. Ahmed, "Analysis of Phase-Locked Loop Acquisition: A Quasi Stationary Approach IEEE, International Conv. Record, 1966, Part 7, Volume 14.

D-5. Goldman, S. L., "Second Order Phase-Lock Loop Acquisition Time in the Presence of Narrowband Gaussian Noise," IEEE Transaction on Communications, April 1973.

D-6. Lewis, J. L., "Probability of Acquisition in the LM Fine Tracking Loop," TRW IOC No. 7131.57.2, 19 December 1972.

D-7. Stiffler, J. J., Theory of Synchronous Communications, Prentice-Hall, Inc. Englewood Cliffs, New Jersey, 1971.